

Cancer Cell Mechanics in Chemoresistance and Chemotherapeutic Drug Exposure

by

Rochelle Smith



Thesis presented in fulfilment of the requirements for the degree of Master of Science in Medicine in Mechanobiology in the Faculty of Health Science at University of Cape Town

Supervisor: Prof T. Franz, Division of Biomedical Engineering (UCT)
Co-supervisor: Prof M. Zaman, Department of Biomedical Engineering (Boston University)
Co-supervisor: Prof S. Prince, Division of Cell Biology (UCT)

Department of Human Biology
Faculty of Health Science
February 2019

The copyright of this thesis vests in the author. No quotation from it or information derived from it is to be published without full acknowledgement of the source. The thesis is to be used for private study or non-commercial research purposes only.

Published by the University of Cape Town (UCT) in terms of the non-exclusive license granted to UCT by the author.

DECLARATION

I, Rochelle Smith, hereby declare that the entirety of the work contained therein is my own, that I am the sole author thereof, that reproduction and publication thereof by University of Cape Town (UCT) will not infringe any third party rights and that it has not been submitted in part or in full for any other degree or qualification to any other University or academic institution.

Signed by candidate

R. Smith

8 February 2019

Date

ABSTRACT

Cancer remains a problem worldwide as one of the leading causes of morbidity and mortality. Many cancer patients experience recurrence and ultimately death due to treatment failure or the development of chemoresistance. The concept of chemoresistance however is complex, recent studies have highlighted that cellular structure and extra-cellular composition, mechanics and structure play a role in the development of chemoresistance. The mechanical properties of cells impact their architecture, migration patterns, intracellular trafficking and many other cellular functions. Studies have also revealed that cellular mechanical properties are modified during cancer progression. We investigated these mechanical properties and changes to them by using a malignant melanoma cell line (WM1158) and a chemoresistant malignant melanoma cell line (SK-MEL29). Malignant melanoma was the cell line of choice as it is one of the most prominent types of cancer known to develop chemoresistance. The aim of this study was to identify the effects of chemotherapeutic drug exposure on the mechanical properties and cytoskeletal composition of drug sensitive and drug resistant malignant melanoma cells. To achieve this, a combination of Multiple particle tracking microrheology (MPTM), quantitative RT-PCR and Western blotting techniques were utilised to demonstrate changes in cytoskeletal elements that are responsible for cellular mechanics. MPTM was developed as an approach to map intracellular mechanical properties of living cells and track the intracellular particles by Brownian motion to establish a viscoelastic model and compare it with the power-law approach. A quantification of the MPTM allowed capturing of the cell stiffness using the mean squared displacement (MSD) of cell under different conditions. The cytoskeletal elements actin and β -tubulin were analysed in qRT-PCR and Western blot as they form the key elements governing a cell's mechanical stability and response to mechanical stimuli. The findings from this study revealed cell stiffness decreases as cancer progress, thereby cells become stiffer. The same pattern was evident for chemoresistant malignant cells and revealed that they had a loss of elasticity in comparison to their counter non-resistant malignant cells. With regards to protein levels and mRNA expression, the chemotherapeutic drug affected the cytoskeleton causing cells to undergo morphological changes which, however, was not seen in chemoresistant cells. The results from this study indicated that measuring mechanical properties of cells provides an efficient marker for cancer diagnosis and deeper understanding of cancer mechanobiology.

DEDICATION

This work is humbly dedicated to all whom are suffering from cancer or have been affected by cancer in any form

To the Person who came and changed everything

and

Most of all to the one who gives me a chance to live, gives me strength and faith to overcome all difficulties,

our

HEAVENLY FATHER

I can do all things through Christ who strengthens me - Philippians 4:13

ACKNOWLEDGEMENTS

I would like to express my deepest and sincerest gratitude to my supervisor Prof Thomas Franz for his support, encouragement and guidance throughout my work. I am grateful that he has introduced me to the field of cell mechanics and for providing me with continuous support, valuable opinions and insight, and priceless guidance over the past few years which has allowed me to expand my ideas and move in the right direction. As well as guiding me along the way in developing Particle Tracking Microrheology at the University of Cape Town.

I would like to acknowledge Prof S. Prince at University of Cape Town for providing access to the Prince laboratory for the completion of molecular experiments and guidance in the development of my study design. I am also grateful to Prof M. Zaman for introducing us to this study and providing necessary information and guidance to perform this study.

I would also like to acknowledge Dr Jade Peres and Mrs Desire Bowers for assisting me in both physical and biological aspects of my experiments. A Special thanks to Mrs Susan Cooper for assistance with my bioengineering experiments and the Human Biology department for their friendship for making the experience all more enjoyable.

A special thanks to Sloan Kettering Memorial for providing me with the necessary chemoresistant cell line to achieve my objectives for this study and their guidance and support with the maintenance and requirements of these cells.

Last but not least, I am immensely grateful to my special person Pierre Woudberg, who has been my ultimate support throughout my studies, for guidance, motivation and understanding. Thank you for standing by my side through the ups and downs, for believing in me when I lost my spark and always reminding me to put on my “uniform”. I will forever be grateful.

CONTENTS

DECLARATION	ii
ABSTRACT	iii
DEDICATION	iv
ACKNOWLEDGEMENTS	v
CONTENTS	vi
LIST OF FIGURES	ix
LIST OF TABLES	xii
CHAPTER 1: Literature Review	1
1.1 Introduction.....	1
1.2 Cancer.....	2
1.2.1 Cancer Defined	2
1.2.2 Types of Tumours	3
1.2.3 Cancer Genetics	3
1.2.4 Tumour Biology.....	8
1.3 Cell Mechanics	10
1.3.1 Cell Mechanics Theory.....	10
1.3.2 Measurement of Cell Mechanical Properties	11
1.3.3 Microrheology for Cell Mechanics Measurement.....	12
1.4 Chemotherapy.....	15
1.4.1 Chemotherapy Explained	15
1.4.2 The Cell Cycle.....	16
1.4.3 Types of Chemotherapeutic Agents	18
1.4.4 Classification of Chemotherapeutic Agents	19
1.5 Chemoresistance.....	20
1.5.1 Chemoresistance Defined.....	20
1.5.2 Factors Affecting Cancer Cell Sensitivity	21
1.6 Aims & Objectives	22
CHAPTER 2: Materials and Methods	23
2.1 Study Design	23
2.2 Cell Lines and Culture	24
2.3 Mycoplasma Test	24
2.4 Seeding Densities.....	25
2.5 Cisplatin Treatment	26

2.6 Cell Morphology.....	27
2.7 Microrheology.....	27
2.7.1 Multiple Particle Tracking Microrheology.....	27
2.7.2 MDS and complex shear modulus calculations.....	28
2.8 Western Blot.....	29
2.8.1 Cell harvest and lysate preparation.....	29
2.8.2 Sodium dodecyl sulphate-polyacrylamide electrophoresis (SDS-PAGE).....	29
2.8.3 Western blot analysis.....	30
2.9 Quantitative Real Time PCR (qRT-PCR).....	31
2.9.1 RNA isolation.....	31
2.9.2 Determination of nucleic acid concentration.....	31
2.9.3 cDNA synthesis for RT-PCR.....	31
2.9.4 Synthetic oligonucleotide primers for qRT-PCR.....	32
2.9.5 qRT-PCR.....	32
2.10 Data and Statistical Analysis.....	33
CHAPTER 3: Results.....	34
3.1 Morphology study to assess cytotoxic effect and confirm chemoresistance.....	34
3.2 Cell mechanical properties obtained by multiple particle tracking microrheology.....	35
3.2.1 Non-resistant Cancer Cells without Treatment.....	36
3.2.2 Chemoresistant cancer cells without treatment.....	36
3.2.3 Non-resistant and chemoresistant cancer cells exposed to chemotherapeutic drugs.....	37
3.2.4 Cancer cell mechanics presented as MSD values.....	39
3.3 Molecular adaption of the cytoskeletal properties of malignant melanoma cells assessed by Western Blot.....	40
3.3.1 Actin protein expression.....	40
3.3.2 β -Tubulin protein expression.....	42
3.4 Gene expression of cytoskeletal properties of malignant melanoma cells assessed by qRT-PCR method.....	44
3.4.1 Actin mRNA expression.....	44
3.4.2 β -Tubulin mRNA expression.....	45
CHAPTER 4: Discussion.....	47
4.1 Morphological Examination.....	48
4.2 Multiple Particle Tracking Microrheology.....	48
4.3 Western blot analysis.....	50
4.4 qRT-PCR analysis.....	51

4.5 Overall Findings.....	52
CHAPTER 5: Conclusion	53
5.1 Future Research.....	53
REFERENCES	55
APPENDICES.....	64
Appendix A: MSK Human Specimen MTA.....	64
Appendix B: Reagents Lists.....	69
Appendix C: Negative controls microrheology (MPTM).....	70
Appendix D: Melting Peak Analysis of Primers for qRT-PCR.....	71

LIST OF FIGURES

Figure 1: Different stages of cancer: A histological illustration of normal cells, benign cell and malignant tumour cells, expressing abnormal cell nucleus as described previously, with permission from (16).	2
Figure 2: Oncogene. An illustration of the process of oncogene activation from proto-oncogene to activation leading to cancer cells, with permission from (43).	6
Figure 3: Tumour suppressor gene. An illustration of the difference between a normal TSG and a mutated TSG with their effects on cell division, with permission from (43).	8
Figure 4: Cancer Development. An illustration of the series of steps of malignant transformation, from initiation stage to metastases as explained above, with permission from (62).	9
Figure 5: The eukaryotic cell. An illustration of the eukaryotic cell with its various components that make up its heterogeneity, including the important factors of the cytoskeleton used to determine mechanical properties of cell mechanics, with permission from (69).	11
Figure 6: Types of chemotherapeutic drug resistance. An illustration of the two types of chemoresistance and the mechanisms of their occurrence due to chemotherapeutic drug exposure, with permission from (112).	21
Figure 7: A flow diagram illustrating the study design of this research.	23
Figure 8: Neubauer chamber and concentration calculation formula. An illustration of the Neubauer cell counting chamber as seen under a light microscope and the standardised cell concentration formula utilised for determining cell densities.	26
Figure 9: Microrheology of biomaterial hydrogelators. (A) Tracer particles are fluorescently labelled. (B) Sample medium with added tracer particles. (C) Video images presenting time-dependant x-y particle trajectories. (D) Particle trajectories pathway are transformed into mean-squared displacement (MSD) profiles and expressed graphically, with permission from (115).	28
Figure 10: Cisplatin cytotoxic effects on WM1158 and presence of chemoresistance in SK-MEL 29. Representative phase-contrast photomicrographs (400x; Olympus 1X71) showing WM1158 and SK-MEL 29 cells treated with Cisplatin at 0 hours (a, b), Cisplatin treatment at 24 hours (c, d), and Cisplatin treatment at 48 hours (e, f), inserted arrows (a, b) indicating white halo of cells undergoing mitosis.	35
Figure 11: Particle Trajectories of WM1158 cancer cells. a) Fluorescence micrograph used for the identification and tracking of particles within the cell, with scale bar representing 20 μm . b) Visualisation of imported trajectories expressing Brownian motion.	36
Figure 12: Particle Trajectories of SK-MEL29 cancer cells. a) Fluorescence micrograph used for the identification and tracking of particles within the cell, with scale bar representing 20 μm . b) Visualisation of imported trajectories expressing Brownian motion.	37
Figure 13: Cisplatin treated cells exposed to mitotracker for determination of mechanical properties of cancer cells. Representative confocal photomicrographs showing WM1158 and SK-MEL 29 cells with positive controls with mitotracker and no treatment (a, b), and Cisplatin treated with concentration IC50 and mitotracker (c, d). Images were captured under a confocal microscope (Zeiss, Germany) at 600x magnification and are representative of a randomly selected field for each condition (scale bars indicate 20 μm). .	38
Figure 14: Particle Trajectories of SK-MEL29 cancer cells exposed to cisplatin. A) Fluorescence micrograph used for the identification and tracking of particles within the cell,	

with scale bar representing 20 μm . B) Visualisation of imported trajectories expressing Brownian motion.	39
Figure 15: Cancer cell mechanics presented as MSD over lag time. A diagram of the ensemble averaged MSD vs lag time for cell lines WM1158, SK-MEL29, and SK-MEL29 IC50 exposed to cisplatin.	39
Figure 16: Power Law coefficient α obtained from MSD values. A diagram portraying the α values of both WM1158 and SK-MEL29 cell lines under the two conditions of Mitotracker exposure only and Mitotracker combined with cisplatin treatment. The MSDs of particle trajectories from the Mitotracker anchored to the mitochondria within cancer cells which exhibits anomalous diffusion dynamics as presented in equation 2 from section 1.3.3.2, $\Delta r^2 t \sim t^\alpha$ (subdiffusive $\alpha < 1$ and superdiffusive $\alpha > 1$).	40
Figure 17: Actin protein analysis. A) Western Blotting of cell extracts from WM1158 and SK-MEL29 visualising actin protein indicated at approximately 42 kDa and normalised to corresponding p38 signals. The conditions for this experiment represent positive (+) as no treatment, IC50 as half the inhibitory concentration dose of cisplatin and 2xIC50 as twice the inhibitory concentration dose of cisplatin. Image J image analysis software was used to quantify signal intensities; these signal intensities are shown in the table below the western blot. B) Successful transfer of proteins onto the membrane and visualized by ponceau stain, serving as normalization for protein loading.	41
Figure 18: Quantification of Actin protein expression. Histogram representing the expressing of relative actin protein concentrations (fold change) throughout the various experimental conditions obtained from Western blot quantification via ImageJ. The conditions for this experiment represent positive (+) as no treatment, IC50 as half the inhibitory concentration dose of cisplatin and 2xIC50 as twice the inhibitory concentration dose of cisplatin, with error bars representing the STDEV. Asterisks indicated statistical significance of treated conditions compared to the non-treated control of the same cell line.	42
Figure 19: β-Tubulin protein analysis. a) Western Blotting of cell extracts from WM1158 and SK-MEL29 visualising actin protein indicated at approximately 50 kDa and normalised to corresponding p38 signals. The conditions for this experiment represent positive (+) as no treatment, IC50 as half the inhibitory concentration dose of cisplatin and 2xIC50 as twice the inhibitory concentration dose of cisplatin. Image J image analysis software was used to quantify signal intensities; these signal intensities are shown in the table below the western blot. b) Successful transfer of proteins onto the membrane and visualized by ponceau stain, serving as normalization for protein loading.	43
Figure 20: Quantification of β-Tubulin protein expression. Histogram representing the expression of relative β -Tubulin protein concentrations throughout the various experimental conditions obtained from western blot quantification via ImageJ. The conditions for this experiment represent positive (+) as no treatment, IC50 as half the inhibitory concentration dose of cisplatin and 2xIC50 as twice the inhibitory concentration dose of cisplatin, with error bars representing the STDEV.	44
Figure 21: qRT-PCR estimated mRNA concentration. Bar graph illustrating the relative normalised mRNA concentration for WM1158 and SK-MEL 9 cell lines. Primers specific to actin (ACTC1) was used and in both indicated cell lines, mRNA levels were first normalised to GUSB and then expressed relative to actin. The conditions for this experiment represent positive (+) as DMSO only no cisplatin treatment, IC50 as half the inhibitory concentration dose of cisplatin and 2xIC50 as twice the inhibitory concentration dose of cisplatin, with error bars representing the STDEV.	45

Figure 22: qRT-PCR estimated mRNA concentrations. Bar graph illustrating the relative normalised mRNA concentration for WM1158 and SK-MEL 9 cell lines. Primers specific to β -Tubulin (TUBB) was used and in both indicated cell lines, mRNA levels were first normalised to GUSB and then expressed relative to β -Tubulin. The conditions for this experiment represent positive (+) as DMSO only no cisplatin treatment, IC50 as half the inhibitory concentration dose of cisplatin and 2xIC50 as twice the inhibitory concentration dose of cisplatin, with error bars representing the STDEV..... 46

LIST OF TABLES

Table 1: Cell culture media (RPMI 1640), antibiotics and supplements.....	24
Table 2: Hoechst stain mounting media.....	25
Table 3: Formulations for SDS-PAGE separating and stacking gels.....	30
Table 4: Primary antibodies used in Western blot.....	31
Table 5: Settings for Thermal Cycler used for cDNA synthesis.....	32
Table 6: qRT-PCR Primers.....	32
Table 7: Programme for Light Cycler qRT-PCT machine.....	33
Table 8: Regularly used reagents and substances.	69
Table 9: Sample Loading Buffer (2X).....	69

LIST OF ABBREVIATIONS

- APS** - Ammonium persulfate
- CCD** - Charge-coupled device
- CDDP** - Cisplatin
- DEPC** - Diethyl pyrocarbonate
- DMSO** - Dimethyl sulfoxide
- DNA** - Deoxyribonucleic acid
- ECL** - Enhanced chemiluminescence
- FBS** - Fetal bovine serum
- GSER** - Generalised Stokes-Einstein Relation
- GUSB** - β -glucuronidase
- HCl** - Hydrochloric acid
- HRP** - horseradish peroxidase
- IC50** - half maximum inhibitory concentration
- IDL** - Interactive data language
- KCl** - Potassium chloride
- MPTM** - Multiple Particle Tracking Microrheology
- MSD** - Mean-Squared-Displacement
- NaCl** - Sodium chloride
- PCR** - Polymerase chain reaction
- PTM** - Particle tracking microrheology
- qRT-PCR** - quantitative real time - polymerase chain reaction
- RNA** - Ribonucleic acid
- RPMI** - Roswell Park Memorial Institute medium
- SDS** - Sodium Dodecyl Sulphate
- SPSS** - Statistical Package for Social Sciences
- TEMED** - Tetramethylethylenediamine
- T_m** - melting temperature
- TSG** - Tumor Suppressor Gene

CHAPTER 1: Literature Review

1.1 Introduction

Cancer remains a major burden worldwide as one of the leading causes of morbidity and mortality. In 2012, approximately 14 million new cases were recorded with an estimate of 8 million deaths occurring due to cancer (1, 2). The burden of cancer is projected to increase over the next few years to reach an estimated 22 million new cases and 13 million deaths related to cancer by 2030 (1, 3). Although the burden of cancer can be seen on a global scale and subsequently developing countries tend to suffer greatly due to limited resources. Cancer however falls under chronic, non-communicable disease which forms part of a larger epidemiological transition. In addition to the associated cancer risk factors for example diet, tobacco, alcohol, lack of exercise, and industrial exposures, developing countries are burdened by cancers which are attributable to infectious diseases (3). Recent studies have indicated of the total deaths recorded per day due to cancer, over two thirds occur in economically developing countries (1, 4).

The management of cancer is complex, with chemotherapy being one of the standard treatment methods of choice, due to its ability to target local tumours, as well as metastasizing cancers. Chemotherapy is used based on its ability to induce cell death in tumours, however many cancer patients experience recurrence and ultimately death due to treatment failure (5, 6). This is caused by a phenomenon known as chemoresistance. This concept was first presented when bacteria became resistance to certain antibiotics, since then cancer cells have been presenting with a similar mechanism (4, 6, 7). This concept however is far more complex than previously thought, recent studies have highlighted that cellular structure and extra-cellular composition, mechanics and structure play a role in chemoresistance.

This literature review will establish a theoretical framework and provide a general overview of the key areas of this research pertaining to this thesis.

1.2 Cancer

1.2.1 Cancer Defined

Cancer is a collection of distinct illnesses that result due to loss of control in normal cell growth patterns (neoplasia) in the human body leading to abnormal cell development. Normal cells are constantly subject to signals that dictate whether the cell should divide, differentiate into another cell type or die. Cancer is usually caused by mutations in the DNA that activate oncogenes, trigger genetic instabilities or silence tumour suppressor genes (8-11). Under normal conditions cells are able to detect and repair damaged DNA strands. If the damage is too severe and cannot be repaired, the cell will undergo apoptosis (programmed cell death) (10, 12). Previously cancer had been associated with an increase in cell number or mutations leading to alterations in regulation of cell production or proliferation mechanism. However in certain cancer types it is caused by decreased apoptotic rates (10).

These abnormal cells are known as tumour cells and are best described as cells that are not responsive to normal growth –controlling mechanisms (13, 14). As tumour cells develop and accumulate, they form masses or lumps known as neoplasms. This neoplastic growth process can be a rapid or slow process (weeks or even years) to develop. The exact growth rate has not yet been established and depends on the type of cell or tissue involved. The tissue pathology varies greatly in the detection from normal tissue, some are obvious and easily visualized, while others are difficult and not that easy detected (8, 9, 15). However, the key element to look out for is an abnormal cell nucleus as the nucleus is the main characteristic feature of a cell and the genetic make-up (DNA) of the cell. There are different stages in cancer development and not all tumours are found to be cancerous. An illustration of normal, benign and malignant cells can be seen in Figure 1 below.

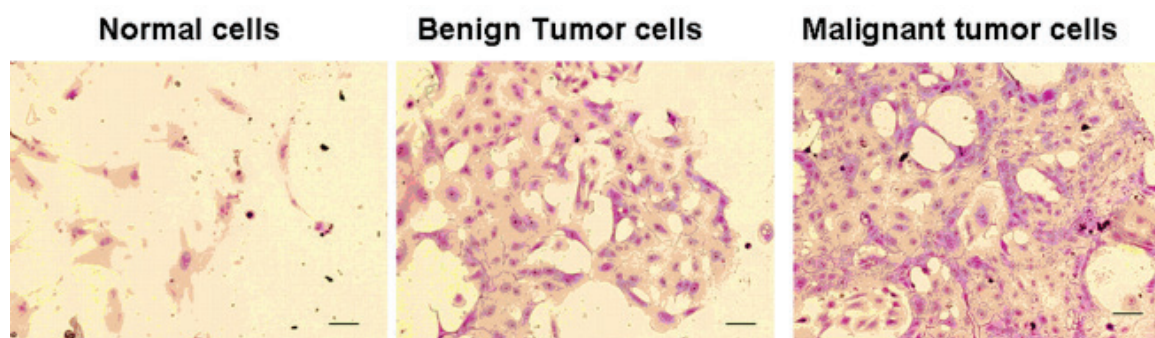


Figure 1: Different stages of cancer: A histological illustration of normal cells, benign cell and malignant tumour cells, expressing abnormal cell nucleus as described previously, with permission from (16).

1.2.2 Types of Tumours

Benign tumours are non-cancerous localised lesions. They are usually small, not reaching larger than 5 cm in diameter. They are also known to be superficial with about only 1% of these lesions being deep (17, 18). Benign tumours have a non-invasive characteristic, therefore when they arise in tissues such as epithelial or mucosal; they grow outwards away from the tissue surface. This outwards growth resembles a polyp which may be either sessile or stalked. Even though these tumours are not capable of spreading or invading other organs or parts of the body, they can be dangerous and cause clinical problems (17-19). These problems are usually caused by fluid flow obstruction (e.g. benign epithelial tumour arising in a duct) or pressure on adjacent tissues (e.g. benign meningeal tumours causing epilepsy). Benign tumours are usually treated by surgical removal and are therefore non-recurring (18).

Malignant tumours however are cancerous lesions and found to be larger and deeper than benign tumours. They are significant in that they are fast growing and have the ability to invade their surrounding tissues (18-20). The fact that these types of tumours can metastasize to other parts of the human body and colonize these distant organs makes them malignant (cancerous). The type of tumour that forms depends on the type of cell that was initially altered (19, 20). There are four types of tumours:

1. Carcinomas - result from altered epithelial cells.
2. Sarcomas - result from changes in muscle, bone, fat, or connective tissue.
3. Lymphoma – a cancer of the lymphatic system cells that derive from bone marrow.
4. Myelomas - cancers of specialized white blood cells that make antibodies.

A tumour can be classified as “cancer” or “malignant” once it has invaded surrounding tissue known as metastasis (12, 21).

1.2.3 Cancer Genetics

Cancer is said to be genetic disease, as it is caused by mutations in critical cancer-susceptible genes (22, 23). Even though other aspects such as environmental factors (carcinogens) or non-genetic factors play a role in many stages of cancer development, a mutation has to occur for a cell to become cancerous (24). Human genes are found in the DNA in each cell in the human body. They are responsible for normal functions of the cell such as, growth rate, proliferation and differentiation, and cell survival. Most of the mutations occur and are accumulated during the division of cells in the normal cell cycle process (25, 26). A mutation

in one gene however is not sufficient for cancer to develop, multiple mutations are necessary for abnormal cells to become cancerous (27).

Cancer has a large genetic component to it; this is because cancer arises from alteration or changes in the DNA of normal cells or by transcriptional or translational processes that then produce mutations in gene expression (27, 28). Genetic changes responsible for the increased risk in cancer development may occur as either a germline and/or a somatic event. Not all cancers are hereditary (genetically inherited), however over 200 hereditary cancer syndromes have been described to date. Germline mutations are inherited genetic changes from an individual's parents that have the mutation present in their germ cells (29, 30). These are the reproductive cells of the body such as ova and sperm and the mutation will be present in every cell of the offspring. These individuals are at a higher risk of certain predisposing malignancies and the risk is even greater if multiple members of the family is afflicted (26, 28).

Somatic mutations are acquired genetic changes occurring during an individual's lifetime and therefore not from genetic inheritance. They arise due to minor sequence changes leading to activation or inactivation of certain gene functions and gene expression or due to exposure to DNA damaging carcinogens (29, 31, 32). The mutations caused by activation that result in the foundational stages of carcinogenesis are found to be mostly somatic events. This type of event can be referred to as an event or mutation caused by some sort of outer stimuli such as environmental factors or carcinogens (28). Even though most of the mutations are caused by somatic events; both types of mutations occur in the cancer-susceptible genes. These genes are classified as oncogenes and tumour suppressor genes (23, 30, 32).

1.2.3.1 Proto-oncogenes

The process whereby cells undergo maturation, differentiation and apoptosis occurs in an orderly fashion. The process is essential in normal human development and also for maintaining the structure and composition of organs and tissues (33). This process is tightly regulated by the genes known as proto-oncogenes. Proto-oncogenes can be found within a cell's nucleus and code for proteins that assist in cell growth regulation. They promote cell growth by contributing to signalling pathways, these pathways are responsible for relaying growth stimulating signals to the cell's nucleus. Proto-oncogenes communicate these signals by a means of intracellular biochemical signals functioning in a cascade (34, 35). This process then results in the activation or repression of certain specific genes.

Proto-oncogenes operate as a positive growth regulator and a mutation in these genes results in a different protein being produced, which in turn interferes with the normal regulation of cells (35, 36). Once the developmental process is completed which they regulate, their activities are then inactivated. If their activity remains at a high or they are later in life inappropriately activated they become mutated. Proto-oncogenes are targets for potential mutations due to their location often being near the breakpoints on chromosomes (35). This leads to them having an increased probability of becoming activated and mutated.

1.2.3.2 Oncogenes

Oncogenes are the mutated form of proto-oncogenes and their inheritance is found to be dominant in nature. A mutation or translocation in a proto-oncogene activates it to evolve into an oncogene; the transcription produces proteins encoded for by the oncogenes. These proteins are either increased or an alteration occurs in the protein itself changing its structure or function (37). This increase or alteration then leads to a decrease in cell differentiation, increase in cell division and an inhibition of cell death therefore resulting in a gain in function (33). Mutations or translocations occur as initiating events for tumour development or during the progression stages, whereas the amplification of oncogenes takes place only during the progression of tumours (38).

Each oncogene is closely associated with the normal DNA sequence found in the cellular genome. The conversion of proto-oncogenes to active oncogenes occurs via one of five mechanisms (39, 40). The first mechanism being due to the overexpression of proto-oncogenes and occurs due to acquisition of a novel transcriptional promoter. The oncogene becomes active as their transcript production occurs at a higher level than those of normal proto-oncogenes. The second mechanism is over-expression and due to proto-oncogenes being amplified. The third mechanism is due to influences of transcription levels, thereby influencing the amount of gene product. Following chromosomal translocation, juxtaposition of oncogenes and immunoglobulin domains occurs, resulting in deregulation of the gene is known as the fourth mechanism. Lastly, activation can occur due to an alteration in the oncogene proteins structure (39-41).

Upon activation of cellular oncogenes, the cell carrying the mutation develops a growth advantage or increased survival (39). These activated oncogenes can represent one of two types of distinct genetic changes, these genetic alterations lead to either an increase in gene expression or an uncontrollable activity of the proteins encoded by the oncogenes (38, 41, 42). The mechanism by which oncogenes are activated is diverse and includes the upregulated expression of gene products. It also includes the expression of mutant protein,

expressing enhanced stability, altered functionality, altered recruitment or subcellular localization of a normal gene product. This expression can be seen through the interaction with an aberrantly expressed or mutant binding protein partner (36, 41).

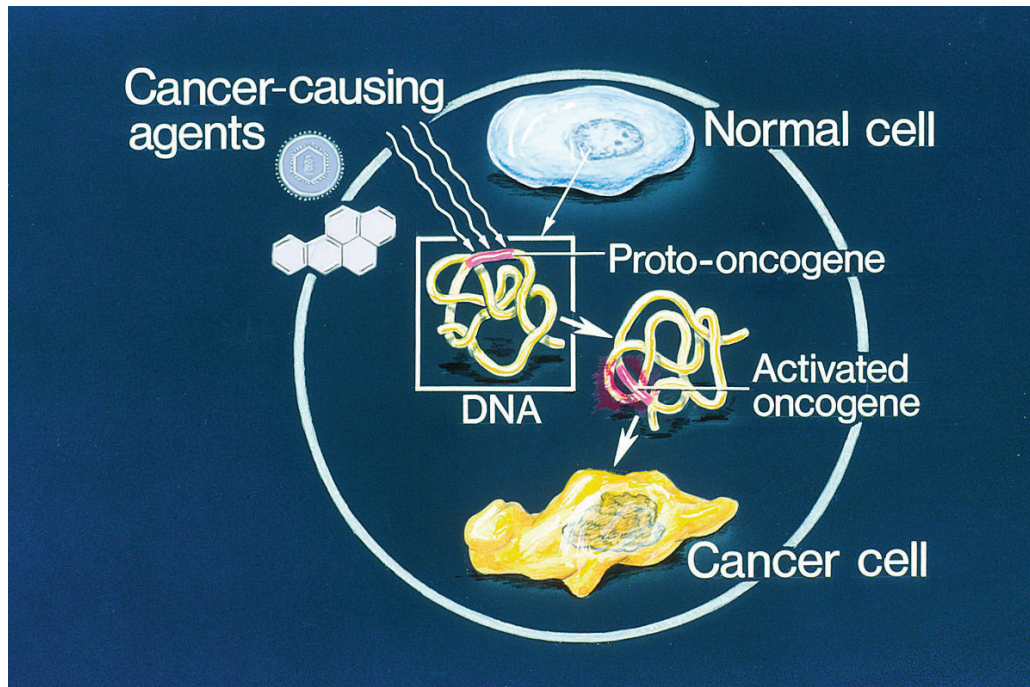


Figure 2: Oncogene. An illustration of the process of oncogene activation from proto-oncogene to activation leading to cancer cells, with permission from (43).

1.2.3.3 Tumour Suppressor Genes

Tumour Suppressor Genes (TSG) also referred to as anti-oncogene, is a class of genes involved in the normal regulation of cell growth, but may become cancer-causing when damaged or inactivated (44-46). They encode for certain proteins that play a part in the inhibition of cell proliferation process. These proteins are crucial to the normal cell development and differentiation process, their products therefore negatively regulate cell growth. It does this by physically blocking the action of growth promoting proteins, thereby representing the opposite side of normal cell growth control (44, 46-48). These proteins therefore inhibit the cell proliferation process or survival and some have been seen to directly antagonize proto-oncogenes action in growth regulation (49). However, some of the tumour suppressor genes have been found to normally be active transcription factors within the nucleus of the cell.

The function of TSG in the cell cycle is to induce checkpoints, pauses or arrests in certain stages of the cycle as needed. This function is to allow for the repair of DNA and acts to ensure that the cell's genome integrity stays intact (42, 45, 50). Therefore, abnormal repression or

inactivation of the TSG is responsible for the deregulation of the cell cycle resulting in excess cellular proliferation by prolonging proliferation signals or cellular disorganisation. Because of this regression of TSG, tumour development is initiated via the elimination of negative regulatory proteins (50, 51). This ability leads to the uncontrolled growth of cancer cells and development of a cancerous tumour, due to the genetic damage or mutation. In some cases, TSG have been found to inhibit the same cell regulatory pathways that oncogenes products have stimulated (46, 50, 51).

The difference between TSG mutations to other potential carcinogenic mutations is that the altered TSGs produce direct modifications in the protein products responsible for the transformed phenotype (46, 50, 51). Proto-oncogenes on the other hand produce indirect effects on the protein products. On a cellular level TSGs behave recessively however their inheritance is dominant in contrast to other cancer related genes. The suppression of TSGs occurs more frequently than the activation of oncogenes (51). Fully functional TSGs are able to suppress tumour development even in the presence of active oncogenes. This indicates the importance of TSGs in the functionality and regulation of normal cells.

It is now evident that oncogenes and TSGs play a critical part in the development of cancer due to their involvement in the activation and inhibition of the cell proliferation process (45, 47). As mentioned previously cancer development is a multistep process in which normal cells or eukaryotes progress from benign to malignant. The complete sequence of events is however not known yet, but it is clear that the activation of oncogenes and inactivation of tumour suppressor genes are critical steps in tumour initiation and progression (45, 48, 51). Oncogenes and TSG cannot trigger cancer development by themselves and therefore jointly play a part in cancer development by combining their functions. Based on this, it is evident that cancer has a genetic component attached to it and can thereby be either inherited or caused by somatic mutations (44, 46, 48).

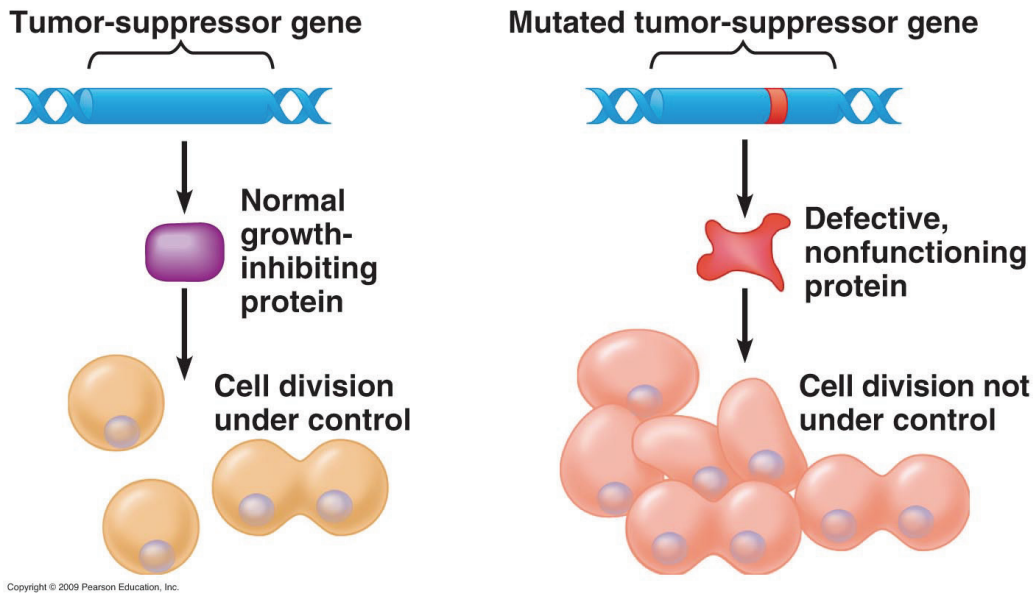


Figure 3: Tumour suppressor gene. An illustration of the difference between a normal TSG and a mutated TSG with their effects on cell division, with permission from (43).

1.2.4 Tumour Biology

Cancer develops from healthy cells in a complex process called malignant transformation. Cancerous cells are known to behave in an independent manner, with loss of growth control forming tumours, this process consists of a series of steps (52-54). The first step in the cancer development is termed Initiation. In this stage cells undergo hyperplasia, being an overproduction of cells due to uncontrolled cell division. Hyperplastic cells do not undergo any morphological changes and the cells appear normal just in excess amounts.

The initiation phase is caused by change in the cells genetic material (DNA mutations) and may occur completely spontaneous or brought on by carcinogens (cancer causing agents) termed initiators (55, 56). Carcinogens bind covalently to DNA or macromolecules within the cell to cause the mutation. The genetic mutations are permanent damage and any daughter cells produced from the division of the mutated cell will carry forth the mutation.

The second stage of cancer development is termed promotion and cells undergo dysplasia (52). Dysplasia results from further proliferation and the cells begin to undergo abnormal morphological changes. In order for this stage to take effect cells had to be mutated by an initiator, as promoters has no effect without an initiator (55). Promoters affect intracellular pathways that lead to increased cell proliferation by alternatively binding to receptors on the cells surface.

In the third stage tumours start to take on form and are termed neoplasms or benign tumours. This process is termed progression and caused by additional changes to the cells (53, 55).

The cells morphological profile is even more disrupted and the cells spreading ranges over a wider area of the surrounding tissue. These tumours however are still contained within their original location and also known as “*in situ*” (53, 57). They are not malignant but considered potentially malignant. The cells of these tumours are termed anaplastic, due to the loss of their original function (57). The loss of original function is associated with karyotypic changes, causing all tumour cells to have an aneuploidy (incorrect chromosomal count) karyotype (55). This change is coupled with invasiveness and alterations in the cell’s biochemistry and morphology.

The last step in the cancer development process is termed metastasis and cells are then considered malignant. In this stage cancerous cells break free from the original/primary tumour site and migrate to other locations in the body in a unidirectional way. The first stage of the metastasis process occurs when primary tumour cells start to invade the tissues surrounding the primary tumour (58, 59). These cells then acquire the correct capacity enabling them to evade the body’s immune defences. The cancer cells are then able to enter circulation. However, before the cancer cells leave their primary site, the primary tumour may have primed pre-metastatic sites. These sites are then more receptive of the arriving tumour cells (60, 61). These processes of tumour biology are depicted in Figure 4 below.

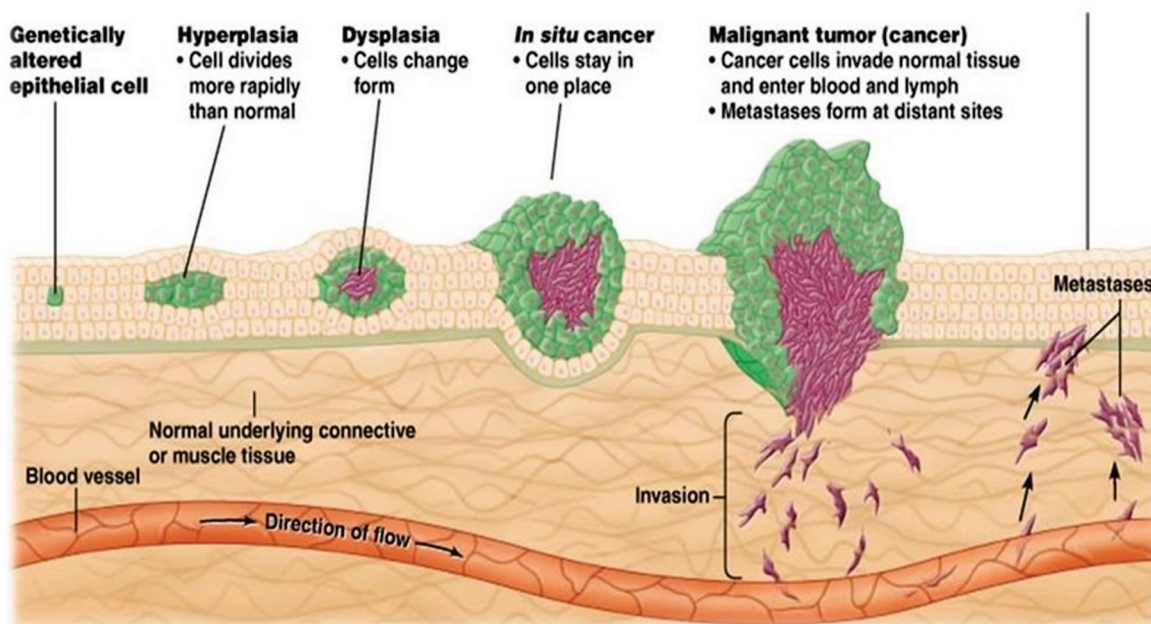


Figure 4: Cancer Development. An illustration of the series of steps of malignant transformation, from initiation stage to metastases as explained above, with permission from (62).

Cancer cells that have detached from their primary sites can metastasize (enter circulation) by either entering the bloodstream or the lymphatic system. Because these systems circulate all over the body it allows the cancer cells to be transported to distant anatomic locations away

from the original sites. Once the cancer cells enter these systems, they are able to leave the system and invade other tissue types if the conditions are favourable (59, 63, 64). Other tissue types that are easily invaded are tissues such as brain, lung, liver and bones. Cancers that have metastasised are secondary tumours and these cancers retain their name from the original cancer. Metastasis plays an important role in the determination of the staging of tumours as well as the treatment of cancers (58).

1.3 Cell Mechanics

1.3.1 Cell Mechanics Theory

The cell is considered to be the basic structure and fundamental unit of life. The human body is made up of 50 to 100 trillion cells termed Eukaryotes meaning “true nucleus”. These cells are a well-organized system that makes up the elements of a fully functioning human body (65, 66). Cells are highly dynamic entities that are made up of a variety of components each with different biomechanical properties and characteristics. They are responsible for all the essential tasks such as replicating, respiring, eating and the excretion of waste products (67, 68). In general, a cell consists of four major components being cellular membrane, cytoplasm, nucleus and organelles, as shown in Figure 5.

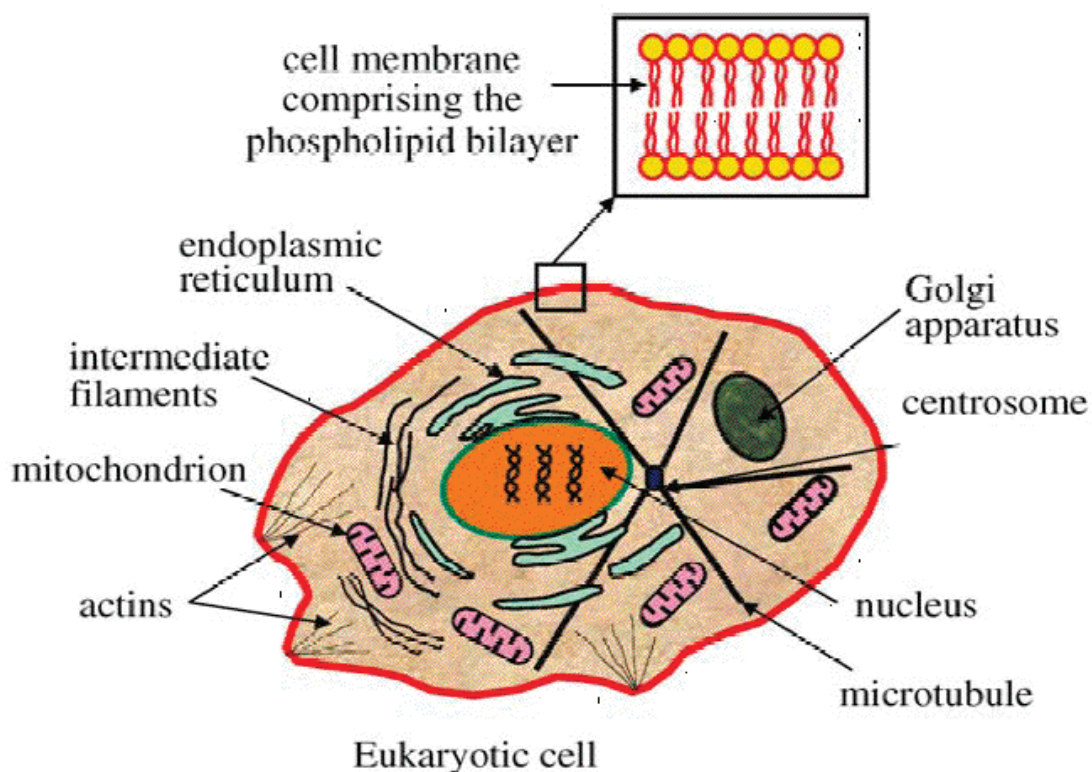


Figure 5: The eukaryotic cell. An illustration of the eukaryotic cell with its various components that make up its heterogeneity, including the important factors of the cytoskeleton used to determine mechanical properties of cell mechanics, with permission from (69).

The cell membrane is the outermost part of the cell and is responsible for maintaining the cells integrity. The membrane is an extremely thin layer allowing the cell to be flexible and somewhat elastic. It also allows cells to communicate and interact with each other by receiving and responding to incoming messages (70). It is also responsible for many important metabolic reactions such as controlling the entry and departure of certain substances. The cytoplasm on the other hand is responsible for most of the cells activity and contains most of the cells organelles (71). The cytoplasm is made by biopolymer filaments such as actin, microtubules, and intermediate filaments, which together make up the cytoskeleton of the cell (70, 72). The cytoskeleton is the supportive framework and can be defined as “a spatially sparse tangled matrix of rods and rod-like elements held together by smaller proteins, which maintains the cell’s structure” (73).

Cells are able to constantly remodel their internal structure in response to chemical and physical stimuli; this remodelling in turn affects their mechanical properties (74). The mechanical properties of a cell depend on the properties of the cytoskeleton and are described in terms of the cells strain response to applied stress or forces. These properties have been found to differ at different length and time scales. Several studies have been conducted to measure mechanical properties of the cytoskeleton with the focus as either using living cells or a reconstituted polymer network *in vitro* (mimicking the cell’s cytoskeleton) (75-78). Two different mechanical behaviours for cells have thereby traditionally been described by investigators and taken from engineering and physics and applied to biological systems, these are known as solid-like and liquid-like. A viscoelastic behaviour has also been defined for cells with both liquid-like and solid-like properties, which will be defined later in this literature review (69).

1.3.2 Measurement of Cell Mechanical Properties

Over the past 150 years, the study of cell mechanics has been a growing field of interest. Researchers have been motivated to develop an improved understanding of the structural and mechanical changes such as cell migration and metastasis, adherence or any simple response occurring due to various cellular environments that occur in cells during various biochemical and biological processes (79, 80). A variety of experimental methods have been developed over the years to find the mechanical properties of cells.

The most common technique utilised to date is probing of cells, in which a mechanical perturbation taking the form of either an applied force of deformation on the cell and allowing the cells dynamic responses to be investigated (81). By measuring cell deformations in response to force became the fundamental mechanism behind these approaches. Over the years a consensus has developed that on a large scale cells are soft viscoelastic materials, however at smaller length scales ($< 1\tau$) they are increasingly heterogeneous (79). Based on this previous statement the cell as a whole is considered to be predominately viscous at lower frequencies and more elastic at increased frequencies, nonetheless the exact frequency at which this transition occurs is unclear.

Other techniques also exist such as deformation with micro-plates, micropipette aspiration, atomic force microscopy, magnetic traps and optical tweezers were later developed based on the same principle of deformation response to force (75). Multiple global laboratories have to date successfully utilised these techniques for measuring cell mechanics, however many questions remain regarding the meaning and accuracy of findings by these methods (82).

1.3.3 Microrheology for Cell Mechanics Measurement

Microrheology collectively refers to a family of recently developed techniques to measure the viscoelastic properties of complex fluids and soft materials with relatively high temporal and spatial resolution (83, 84). It uses Brownian motion to assess viscoelasticity. Brownian motion describes the random movement of particles embedded in a system of molecules and is the backbone of particle tracking microrheology. This motion can be quantified and further used to study the mechanical properties of materials. Mechanical properties can be determined by tracking the motion of micron-sized particles embedded in a material. The techniques previously mentioned are known as active microrheology, these techniques use external forces to manipulate probe-particles. Passive microrheology however simply allows the particles to be driven by the thermal energy of the material. Passive methods have an advantage over active methods since no large strain or stress is applied to the cell and a linear response can be measured directly. This is particularly useful in soft materials and complex fluids where even a small-imposed strain can cause reorganization of structure within the material and thus change its viscoelastic properties (e.g., strain hardening or shear thinning) (85, 86).

1.3.3.1 Viscoelasticity

Viscosity is a property of a material that describes the material's resistance to flow as a fluid under the application of a shear stress (stress is the average amount of force exerted per unit area). Elasticity however is thought of as a measurement of deformation in solid material in response to an applied stress or strain. A viscous system is constituents such as Newtonian fluids (e.g. water, glycerol or oil) and is known to lose its shape and dissipate energy in response to a stress through viscous flow. A pure elastic system on the other hand contains solid constituents (e.g. rubber or a bouncing ball) that will retain energy and return to its original shape in a spring-like effect once the stress has been removed (75). A viscoelastic material is therefore a complex material that displays both viscosity and elasticity. This principle is used to study mechanical properties in microrheology and measures complex systems such as cells in response to applied forces.

1.3.3.2 Particle Tracking Microrheology

Particle tracking microrheology (PMT) is a passive microrheology technique that measures the Brownian motion of particles to extract mechanical properties at small scales. This technique that allows for the collection and analyses of the displacement of tracer particles embedded within a medium (80). It is used to investigate viscoelastic properties and provide insight into the structural rearrangements of a wide range of materials, in particular soft materials and complex fluids like cell cytoplasm in living cells. In passive microrheology, no force is applied; the particle displacement is in response only to spontaneous motion of tracer particles (79). This spontaneous motion deforms the medium in the vicinity of the particle. Brownian motion of the particles can then be taken with a light microscope of adequate resolution equipped with a CCD camera to capture a series of magnified video images.

Utilising this technique the displacement of fluorescently labelled tracer particles in the medium due to thermal fluctuations can be measured (87). The video images are processed into time-dependant x-y particle trajectories. By using specialized image processing software and tracking routines, the particle trajectories can be used to quantify the amplitude of motions over different time scales by Brownian motion which is expressed as the Mean-Squared Displacement (MSD). The MSD of the particle's trajectories is used to quantify its amplitude of motion over different time scales. The particle trajectories data is of a stochastic nature and the particle dynamics needs to be statistically analysed. Transforming the particle trajectories into mean-squared displacement profiles provides a convenient way to quantitatively characterize this motion. The MSDs are related to the particle trajectory according to

$$\langle \Delta r^2(t) \rangle = \langle [x(t + \tau) - x(t)] + [y(t + \tau) - y(t)] \rangle^2 \quad [1]$$

In this equation t refers to position in time, and τ to the lag time between the particle positions. In the case of viscoelastic materials, MSDs scale nonlinearly with time according to a power law

$$\langle \Delta r^2(t) \rangle \sim t^\alpha \quad [2]$$

The power law exponent, α , is a representative of the type of motion the particle undergoes. Particles may exhibit locally constraint solid-like motion ($\alpha = 0$), sub-diffusive motion ($0 < \alpha < 1$) at short time intervals, diffusive fluid-like motion ($\alpha = 1$), or enter into the super diffusive regime ($\alpha > 2$) at longer time intervals.

The MSD can be computed using the tracer particles for each individual bead; once the MSD is determined, the generalized form of the Stokes-Einstein Relation (GSER) can be used to extract mechanical properties. Applying the algebraic approximation of the Generalized Stokes-Einstein Relation (GSER), the shear modulus of the medium can be calculated according to the following equation (83):

$$\tilde{G}(s) = \frac{k_B T}{\pi a s \langle \Delta \tilde{r}^2(s) \rangle} = \frac{k_B T}{\pi a \langle \Delta r^2(t) \rangle \Gamma\left(1 + \frac{\partial \ln \langle \Delta r^2(t) \rangle}{\partial \ln t}\right)} \quad [3]$$

In this equation, $\tilde{G}(s)$ is the shear modulus in the Laplace frequency domain, s , k_B the Boltzmann constant, T the temperature of the medium, a the radius of the particle, and Γ refers to the gamma function (83). By replacing the Laplace frequency with the $i\omega$, the complex shear modulus can be expressed by:

$$G^*(\omega) = G' + iG'' \quad [4]$$

In this substitute equation G' and G'' represents the storage and loss moduli, respectively. The amplitudes of the tracer particle motions are thereby inversely proportional to the material's stiffness and directly related to the network's mechanical properties.

1.4 Chemotherapy

1.4.1 Chemotherapy Explained

Chemotherapy or cytotoxic medication is the use of medication or chemicals (such as aspirin or antibiotics) to treat diseases. Although it is more commonly known as the treatment for cancer and more than 100 chemotherapeutic drugs are available today. These therapeutic agents can either be used individually or in a combination to increase these treatment modalities effectiveness (88). These agents vary widely in their chemical composition, mode of action, effectivity for specific cancer types and side effects. In order to understand therapeutic effect of these medications, the progression of cancer and normal cell cycle need to be understood (89, 90). As described previously tumours are made up of cells that are reproducing at abnormally high rates. The normal eukaryotic cell knows when to inhibit reproducing (or dividing) when contact is made with other cells. Tumour cells nevertheless do not have this inhibitory mechanism causing cells to continue dividing and replicating. The RNA or DNA of a cell tells it how to replicate itself, and classic chemotherapy (which excludes immunotherapeutic and biological response modifiers) works by penetrating the cell walls and destroying the RNA or DNA. The chemotherapeutic drugs effectiveness is increased by the replication rate of tumour cells and specific stage of the cell cycle.

Cytotoxic medication works by causing destruction of cancer cells and preventing proliferation of cancer cells (88). The primary objective of using this treatment is to obtain an adequate exposure to cancer cells to obtain reasonable destruction while limiting the unacceptable toxicity to the normal functioning cells of the body (88, 90). Chemotherapy is the main treatment of choice for cancer patients, compared to radiotherapy, immunotherapy and surgery. It has been shown to produce more satisfactory benefits in cancer patients and increase the chance of survival. It was initially introduced as a definitive treatment or as an adjuvant therapy for asymptomatic patients with the aim to alleviate disease progress and improve survival. However, chemotherapy has an added benefit that it is able to act on locally confined tumours as well as metastasized malignancies, leading to increased benefits to later stages of the disease.

1.4.2 The Cell Cycle

A cell undergoes a series of cycles, from the time it forms until it divides and matures; this is known as the cell cycle (91). A newly formed cell will undergo proliferation and then divide into two new cells, known as daughter cells. These daughter cells can then further proliferate and divide into mature differentiated cells (70). However only cells' containing a nucleus (eukaryotes) are able to undergo the process of cell cycling (92). This is due to the fact that a duplication of the cell and its contents such as the organelles and DNA are made during the replication of the cell in the cell cycle.

The events that occur during the cell cycle therefore are understood to correspond to the mitotic cycle (93). Most cells in the body are in a quiescent state, they will only undergo change by activating the cell cycle when there is a definite need. This need is triggered upon a proper mitogenic stimulus for example growth factors (94, 95). The human cell cycle is accomplished in approximately 24 hours and classified into two stages: interphase and mitosis. Interphase is further classified into three major phases: G1 (gap 1), S (DNA Synthesis), and the G2 (gap 2) phase, with mitosis being the M phase (96). Each of these phases has a very specific function that serves to ensure proper cell division resulting in a fully functional daughter cell.

a) Interphase

During interphase the cell grows and maintains its routine functions as well as its contributions to the internal environment. It is described as the phase when the cell accumulates material, nutrients and subsequently doubles its genome (92, 97). Interphase is divided into G1, S, and G2 phases based on the sequence of activities.

b) Gap 1 phase

The G1 phase is known as the gap between the end mitosis and the start of the S phase and is responsible for preparing the cell for DNA synthesis. In this phase the cell is sensitive to positive and negative cues from growth signalling networks (97, 98). However, while this phase may seem relatively uneventful, it is the most important regulatory phase in the cell cycle.

The cell has the ability to decide to either irreversibly enter the cell cycle through mitosis or enter a quiescent phase. This decision making processes is controlled by occurrence known as restriction point (95). The restriction point occurs late in the G1 phase and once the

restriction point has been crossed, a strong commitment to proliferate has been triggered and a round of DNA replication is executed after the G1-S transition (94, 96).

c) S phase

The S phase is the most important stage as this is where DNA synthesis occurs. The initiation of DNA synthesis occurs right at the G1/S phase transition. It is a delicate process whereby the cell's genome is copied, producing an identical copy yielding a single cell with two sets of each chromosome (95, 96). Once this is completed the cell can enter the G2 phase before mitosis can occur.

d) G2 (Gap 2) phase

The G2 phase is the phase between the completion of the S phase and the beginning of mitosis. It is responsible for preparing the cell to enter the mitosis and serves as a buffer to ensure the DNA synthesis process is a complete phase (91). This phase functions in ensuring the required proteins for nuclear envelope breakdown, chromosome condensation, spindle formation, and other processes required for the cell to enter into mitosis are synthesised. DNA synthesis needs to be complete in order for mitosis-promoting functions to be initiated, therefore serving as a buffer phase to prevent premature cell division (96). Once this phase is complete the cell then has two sets of identical chromosomes, cell growth can then continue ensuring the cell doubles in size to allow for division in the mitosis phase.

e) Mitosis

Mitosis consists of four sub stages, each with a specific action guaranteeing the complete separation of daughter chromosomes from the original cell, resulting in complete enclosure of the identical genetic material in the newly formed cells (92, 97). This stage of the cell cycle is an essential step for the maintenance of genome stability (99).

Prophase is the first sub stage, in which the nuclear envelope of the original cell is broken down by the protein synthesised in the G2 phase. The chromosomes are then condensed and spindle formation is initiated (99, 100). This is followed by Pro-metaphase being a transition period allowing the sister chromatids to shuffle around until they are aligned in the middle of the cell (96, 101). This alignment of the chromatids is termed Metaphase. The next sub stage Anaphase is responsible for separating the sister chromatids to opposite poles of the cell. Lastly, the physical division of the cell occurs resulting in the two separate daughter cells and is known as Telophase (95).

f) G0 phase

The G0 phase is known as the quiescent phase or resting phase. It is a state that enables the cells to function properly but not divide. Cells enter this stage when they have reversibly withdrawn from dividing in the cell cycle. This occurs due to mitogen deprivation or in response to a high cell density (95, 98). Most of the adult human cells are in this phase as they are already matured, unless activated by mitogenic stimulus such as tissue damage. However some tissues are constantly in the cell cycle process and this is due to their functionality, for example blood cells or skin cells that are in a constant state of maturation (101). This is strongly related to their on-going aging and limited life span (92).

1.4.3 Types of Chemotherapeutic Agents

As chemotherapeutic agents target cancer cells that are actively replicating, however there are different types, each with a different mode of action. Many act by directly damaging the cell's DNA, interfering with cell division, leading to apoptosis (activated cell death) (102). Others act indirectly by interfering with the cell cycle (mitosis) or affecting the replication of cancer cells by blocking the use of nucleotides required for DNA synthesis (102, 103). These agents are classified based on their mode of action and chemical structure. There are three categories described, these being:

1) Cell cycle phase-specific drugs, they are effective against cells that are active in a particular phase of the cell cycle and target only that specific phase, for example during a growth phase. These types of chemotherapeutic drugs are significant as they act on cancer cells either in the G1 phase or S-G2-M phase of the cell cycle (102). As mentioned previously these are the most crucial steps in the cell cycle and therefore lead to an increased cytotoxic effect on the cancerous cells that are rapidly dividing or are in those specific stages on proliferation. These types of drugs focus mainly on the vulnerability of the cancer cells and thereby have the potential to enable clinical outcomes (104, 105). The only pitfall is that these drugs reach a plateau with respect to their ability to kill cells and therefore an increase in drug dosage will not cause an increase in cell kill once the plateau has been reached (106).

2) Cell cycle-specific drugs are effective against actively proliferating cells in a particular phase, but do not require the cell to be in a specific phase of the cell cycle to be effective. CDKs are certain proteins responsible for the activation of the cell cycle in cancer cells (103, 107). These proteins are found to be over-expressed whereas the cell cycle inhibitory proteins are under-expressed; this leads to uncontrollable growth of cancer cells. The foundation

behind the development of cell-cycle specific chemotherapeutic drugs is to target the over-expressed proteins in cancer progression cells (105). This dynamical approach then causes an inducing inhibitory effect by blocking the cell cycle at the divisional phase. All cells in the cell cycle go through a resting phase and are considered to be in a quiescent state. The limitation seen in these types of chemotherapeutic drugs is that they do not affect cells in the resting stage of the cell cycle (103, 106, 107). Thereby these cells are thought of as being kinetically resistant to these types of chemotherapeutic drugs.

3) Cell cycle–non-specific drugs are effective on cancer cells in any phase of the cell cycle, but mainly target cancer cells in the resting (G0) phase of the cell cycle. These chemotherapeutic drugs are active to any phase of the cell cycle. They have been found to be most effective against slow growing tumours as they mainly target quiescent cells. Their mode of action occurs as a bimolecular reaction and DNA is the target site for these types of drugs. Due to this fact maximum cell kill volume is not possible when cells are in the S phase of the cell cycle at the time the drugs are administered. These agents have a linear dose-response curve which allows for the greater the dose of drug administered, the greater the fraction of cells killed (106). The action of these drugs are therefore dependant on the drug concentration and the density of the cell (108).

1.4.4 Classification of Chemotherapeutic Agents

Chemotherapeutic agents are further classified into classes based on their action, structure and source. These classes being: Alkylating drugs, Antimetabolites and Natural products. Most alkylating drugs fall into the cell cycle–specific category and some are cell cycle–non-specific as they cause DNA damage, enabling replication (102, 109). Antimetabolites act as a substitute for the metabolites that are used in normal metabolism; therefore, most fall into the cell cycle–specific category with some also being phase-specific. The last class being natural products such as antibiotics, mitotic inhibitors, Taxanes and topoisomerase inhibitors, they fall into the any of the three categories depending on the agent (109). As described, there are different types of chemotherapeutic agents all with their own unique actions for damaging cancer cells in different phases of the cell cycle and different ways. It is often difficult to determine the exact phase the cancer cells are at in differentiation, therefore to improve and increase the effectiveness of cancer cell killing a combination of these drugs are often employed (108, 109). This method of drug administration and treatment option is known as combination chemotherapy.

1.5 Chemoresistance

1.5.1 Chemoresistance Defined

Chemotherapy resistance is a phenomenon in human tumours that occur when tumour cells become tolerant to the effects of chemotherapeutic drugs and are mostly evident in advanced metastatic stages of the disease. This concept was first evident in bacterial states, when bacteria were found to become resistant to certain antibiotics (88, 110). Since then similar mechanisms had been found to occur in other diseases, including cancers. The primary cause of chemotherapeutic drug failure in most human tumours has been recognised to be due to drug resistance. Although other factors such as pharmacological factors including inadequate drug concentrations targeting the tumour site and cellular factors, contribute largely to clinical resistance of several tumour types (88, 89). The tendency of malignant cells to acquire mutations causes them to resist the effects of these therapeutic agents, therefore limiting the chemotherapy's effectiveness leading to resistance. It has been found that heterogeneous tumours consisting of mixtures of chemo sensitive and chemo resistant cells initially respond to treatment. The patient then tends to relapse as the chemo sensitive cells undergo apoptosis and the chemo resistant cells remain, becoming predominant (102, 111).

There are two types of distinct manifestations of chemotherapeutic drug resistance referred to as intrinsic (natural) or acquired resistance, illustrated in Figure 1.6 below. They are classified based on the initial response to the first exposure to the chemotherapeutic agent (89, 110, 111). The intrinsic resistance occurs naturally prior to chemotherapy exposure and acquired resistance develops during treatment due to the sensitivity of tumours to the chemotherapy. In acquired resistance the tumour may become cross-resistant to a range of different chemotherapies depending on type and mode of action. However a common cellular base exists, both manifestations develop a simultaneous phenotypic resistance to a variety of structurally and functionally diverse agents (89). The drug resistance is a multifactorial phenomenon that involves multiple unified or independent mechanisms evident in both manifestations.

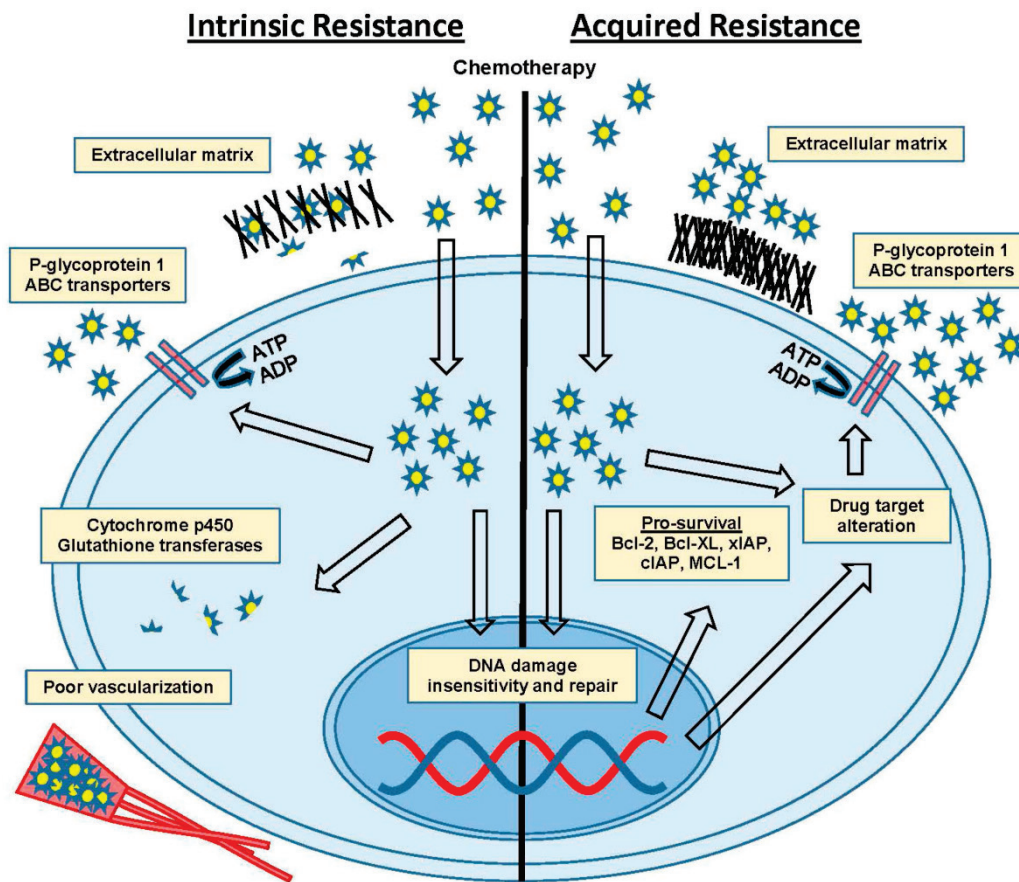


Figure 6: Types of chemotherapeutic drug resistance. An illustration of the two types of chemoresistance and the mechanisms of their occurrence due to chemotherapeutic drug exposure, with permission from (112).

1.5.2 Factors Affecting Cancer Cell Sensitivity

The concept of chemotherapy resistance is complex as numerous factors affect the sensitivity of cancer cells and are grouped based on their main mechanisms. These factors are grouped into three varieties: **(1)** decrease of active drug concentration at target level due to activation of transporter proteins or detoxification mechanisms within the cell; **(2)** alterations affecting drug–target interactions; **(3)** factors influencing the cellular response that affect tumour cell survival (89, 113). With regards to cellular response, the factor that has a major affect is the increased ability of the cell to repair DNA damage or tolerate stress conditions (111). It has been found that some methods of chemotherapy resistance are disease-specific, while others are evolutionarily conserved, such as drug efflux, observed in microbes and human drug-resistant cancers (110, 113). Although many types of cancers are initially susceptible to chemotherapy, over time they can develop this chemotherapeutic drug resistance through these and other mechanisms, such as DNA mutations and metabolic changes that promote drug inhibition and degradation (110). Therapeutic failure is largely due to the heterogeneous

nature of most cancers which is a result of increased diversity of resistant phenotypes (111, 113). Resistant cancer phenotypes become more aggressive over time and exposure to chemotherapeutic agents lead to poor clinical outcomes and decreased survival rates in patients.

1.6 Aims & Objectives

AIM:

To identify the effects of chemotherapeutic drug exposure on the mechanical properties and cytoskeletal composition of drug sensitive and drug resistant malignant melanoma cells. This dissertation explores the hypothesis that exposure to a chemotherapeutic drug leads to a change in intracellular stiffness of malignant melanoma cells. Intracellular stiffness will be assessed by Actin and β -Tubulin as intracellular indicators.

OBJECTIVES:

Objective 1: To determine the mechanical properties and cytoskeletal composition of chemosensitive malignant melanoma cells (WM1158). This will be achieved via Passive based Multiple Particle Tracking Microrheology (MPTM) to capture the mechanical properties and Western Blotting and qRT-PCR techniques to examine the cytoskeletal composition using Actin and β -Tubulin.

Objective 2: To investigate intracellular stiffness via MPTM, biochemical properties via Western blotting and mRNA via qRT-PCR of chemoresistant malignant melanoma cells (SK-MEL 29).

Objective 3: To identify intracellular stiffness and cytoskeletal composition changes of chemosensitive (WM1158) and chemoresistance (SK-MEL 29) malignant melanoma cells exposed to Cisplatin a chemotherapeutic drug. The data obtained will be compared to Objective 1 and 2 to achieve the aim of this study.

CHAPTER 2: Materials and Methods

The following chapter describes the materials and methods for cell culture, multiple particle tracking microrheology (MPTM), molecular biology techniques and data analysis.

2.1 Study Design

This was a quantitative research, which utilised a combination of microrheology and molecular biology techniques to identify a linkage between chemoresistance and the cellular mechanics of cancer cells. A flow diagram demonstrating the study design is presented in Figure 7 while detailed descriptions of protocols used in this study is provided below.

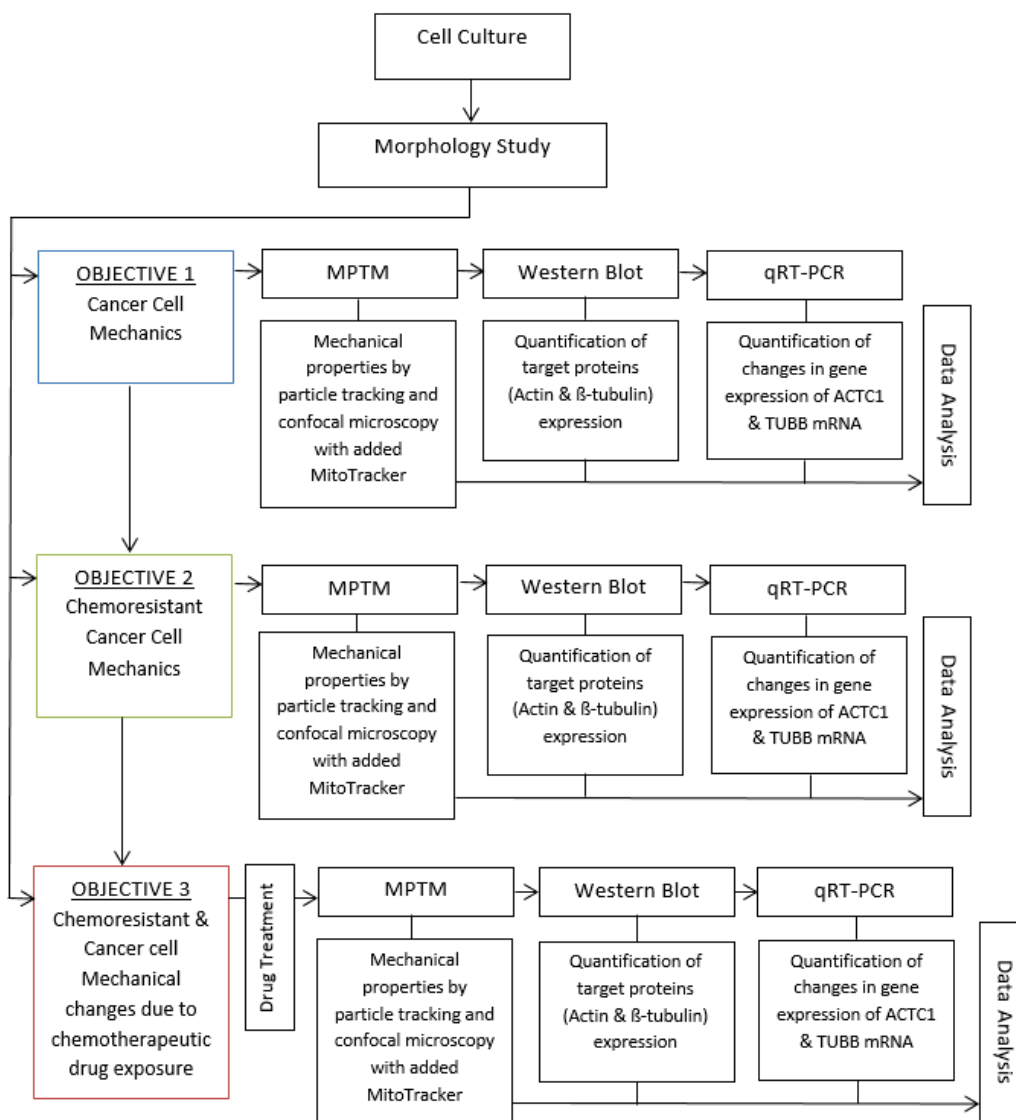


Figure 7: A flow diagram illustrating the study design of this research.

2.2 Cell Lines and Culture

Two cell lines were used in this study. The WM1158 is a metastatic human derived melanoma cell line with mesenchymal morphology. This cell line was obtained by Prof S. Prince (Department of Human Biology, Prince Laboratory, University of Cape Town, SA). The cell line SK-MEL 29 is a human derived resistant metastatic melanoma cell line that was purchased from Memorial Sloan-Kettering Cancer Centre, New York, USA.

Cell lines WM1158 and SK-MEL 29 were both cultured in RPMI 1640 medium (Highveld Biological, UK) pH 7.2, supplemented with 10% fetal bovine serum (FBS), 100 U/mL penicillin and 100 µg/mL streptomycin. The cell lines were grown at 37°C in an air-humidified atmosphere containing 5% CO₂ incubator and typically maintained in 10mm dishes in a 10mL volume of media. Cells were routinely passaged once a 80-90% confluence was reached with trypsin (Sigma-Aldrich, USA) centrifuged for 2min at (2000rpm) and re-suspended in fresh medium. Cells were initially subjected to mycoplasma tests and only mycoplasma free cells were utilised in experiments.

Table 1: Cell culture media (RPMI 1640), antibiotics and supplements.

Name of Product	Quantity
ddH ₂ O	1 L
NaHCO ₃	2.0 g
RPMI powder	10.7 g
FBS	50 mL
Penicillin/Streptomycin (PenStrep)	5 mL

2.3 Mycoplasma Test

The mycoplasma test utilises the Hoechst stain which is a nuclei (DNA) staining solution and detects the presence of mycoplasma organisms within a cell culture. Cells were grown on a coverslip in a 35mm culture dish for minimum 24 hours in antibiotic-free medium (RPMI only). Coverslip containing cells were fixed with 1mL 1:3 mixture of glacial acetic acid and methanol (fixing solution) for 10sec x2, washed x3 gently with water to remove the fixing solution and air-dried at room temperature until dried (\pm 5min). Once dried, the DNA was stained with 0.5 µg/ml Hoechst Stain (Sigma, St Louis, MO, USA) for 10 sec, briefly washed x3 with water to remove excess stain and then mounted on a slide with mounting fluid (see Appendix B). The cells were immediately viewed using a fluorescence microscope. Mycoplasma negative cells

stained positive with Hoechst stain only in the nucleus, while cells infected with mycoplasma showed staining in both the nucleus and the cytoplasm.

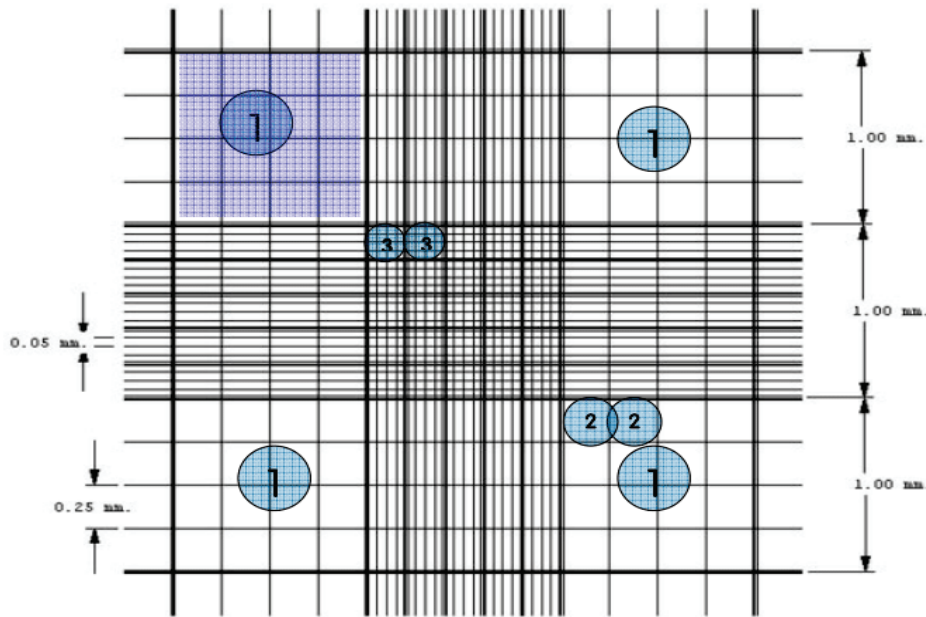
Table 2: Hoechst stain mounting media.

Name of Product	Quantity
0.1M citric acid	22.2 mL
0.2M Na ₂ HPO ₄ .2H ₂ O	27.8 mL
Glycerol	50 mL

Make up to 100mL, pH 5.5, store @ 4 °C

2.4 Seeding Densities

The seeding densities for each experiment were determined by cell counting using a basic haemocytometer (Neubauer Chamber, Celeromics, Spain). Trypsinised cells were centrifuged at 2000rpms for 2min into a cell suspension. 10µL cell suspension was introduced between the glass coverslip and Neubauer chamber central area. A light microscope was used to perform the count, the four larger squares of the Neubauer chamber were counted and the average of the four areas was used to determine the concentration of seeding density. The concentration calculation formula as seen in Figure 8 below was used to determine the specific seeding density for both cell lines as indicated in each experiment.



SQUARE 1

$$\text{Area} = 1 \text{ mm} \times 1 \text{ mm} = 1 \text{ mm}^2$$

$$\text{Volume} = 1 \text{ mm}^2 \times 0,1 \text{ mm} = 0,1 \text{ mm}^3 = 1 \times 10^{-4} \text{ ml}$$



$$\text{Cell concentration} = \frac{\text{Total Cells Counted}}{\text{Number of squares}} \times 10.000$$

Figure 8: Neubauer chamber and concentration calculation formula. An illustration of the Neubauer cell counting chamber as seen under a light microscope and the standardised cell concentration formula utilised for determining cell densities.

2.5 Cisplatin Treatment

Cisplatin (CDDP) is a palladium-based compound with potential anti-cancer activities. Based on these properties, Cisplatin was used as the treatment of choice for this study. Pre-prepared Cisplatin (Pfizer, South Africa) dissolved in dH₂O to give a final concentration of 1mM was used for both WM1158 and SK-MEL-29 cell lines. A half maximum inhibitory concentration also known as IC₅₀ value of (4.67µM) and IC₅₀x2 value of (9.34µM) were used in all experiments and was made from the 1mM stock solution. Depending on the required volumes, the IC₅₀ and IC₅₀x2 treatment concentrations were established and both cell lines were treated at these specific concentrations for each experiment. Normal un-supplemented culture media only was used as the vehicle for all experiments as Cisplatin was dissolved in dH₂O and normal culture media contained dH₂O.

2.6 Cell Morphology

WM1158 and SK-MEL 29 cells were plated at 5×10^4 cells/mL and incubated for 24 hours in order to obtain 70-80% confluency on the day of treatment. Morphological changes were monitored by visual inspection and photographed using an inverted light microscope (Olympus 1X71, USA) 4x objective and camera (Zeiss AxioCam, Germany) after CDDP treatment at 0 hours, 24 hours and 48 hours, respectively.

2.7 Microrheology

2.7.1 Multiple Particle Tracking Microrheology

Cells were plated in tissue culture glass-bottom well-plates used for high-resolution imaging and contain no additional substrate coating (Greiner Bio-One, Germany) (83, 114) at a seeding density of 10×10^4 cells/mL in RPMI 1640 no phenol red (Highveld Biological, UK) and incubated for 24 hours until 60% confluence. After 24 hours cells were treated with CDDP and incubated for a further 24 hours. Cells were then exposed to MitoTracker Green FM (Life Technologies, SA) and further incubated for 30min to allow the MitoTracker to diffuse through the cells. Two of the four wells of the culture dish were treated with CDDP; one was left untreated as a positive control and one with DMSO and no MitoTracker as the negative control. Through the course of the experiment cells were kept in an incubator and only removed for imaging sessions. Time lapse images were captured using a confocal microscope (Zeiss AxioCam, Germany) for a total of 90sec at 0.05fps (yielding a total of ± 130 images per time lapse).

These images captured the displacement of fluorescently labelled tracer particles (mitochondria) in the cytoplasm due to thermal fluctuations and were processed into time-dependant x-y particle trajectories (87). The particle trajectories were used to quantify the amplitude of motions over different time scales by Brownian motion which is expressed as the Mean-Squared Displacement (MSD). This method is illustrated in Figure 9.

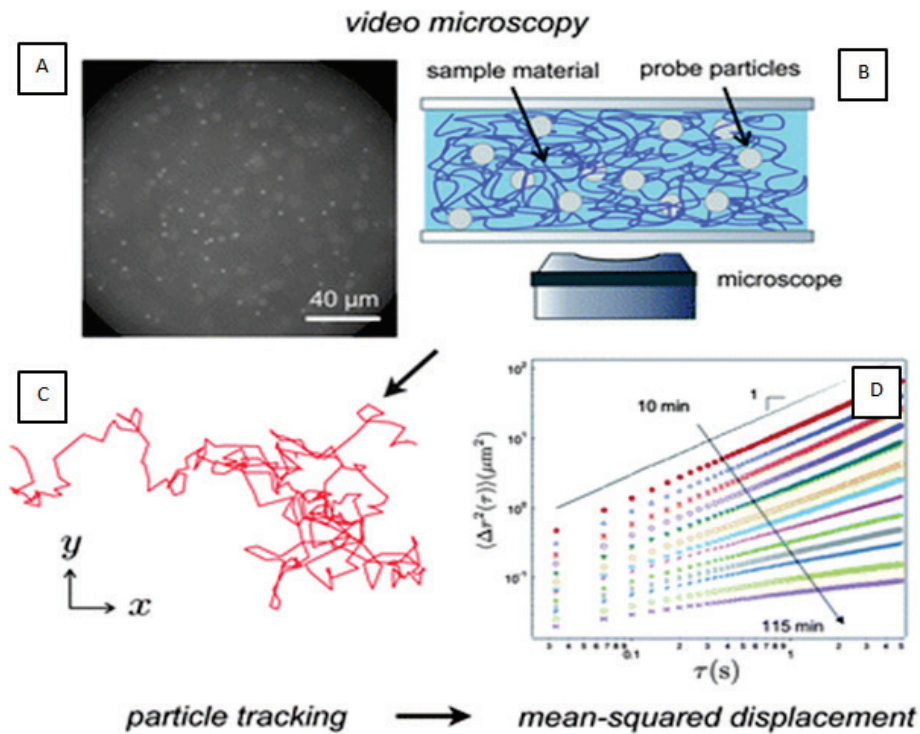


Figure 9: Microrheology of biomaterial hydrogelators. (A) Tracer particles are fluorescently labelled. (B) Sample medium with added tracer particles. (C) Video images presenting time-dependant x-y particle trajectories. (D) Particle trajectories pathway are transformed into mean-squared displacement (MSD) profiles and expressed graphically, with permission from (115).

2.7.2 MDS and complex shear modulus calculations

The captured image sequences from the confocal microscope were used to track the particles individually using MATLAB routines (The MathWorks, Natick, MA). These routines were originally written in IDL by Crocker (116) and ported to MATLAB by Blair (117). The MATLAB routines were utilised to **i)** locate particle positions for each frame, **ii)** filter unwanted tracks or particles that could be caused by digitization errors, table vibrations or noticeable intracellular motor transport motion), and **iii)** link the positions in each frame into tracks for a collection of frames. A MATLAB GUI that was written in-house using the particle tracking routines was used to obtain tracks from all the image sequences. Using the particle-ensemble averaged MSD at each lag-time the mechanical properties of cells were computed. The MSD and complex shear modulus were computed as described by others (77, 117, 118).

The complex shear modulus (also known as the viscoelastic modulus) expresses the elastic modulus as the real (storage) component and the viscous modulus as the imaginary (loss) component. As suggested in previous findings and subsequently demonstrated in a number of studies the GSER was used for estimation of complex shear modulus from MPTM MSD

measurements in complex in live cells (69, 77, 79, 80, 90, 118). The mean of all squared displacements at a given time point for a minimum of 10 tracked particles was used per cell line condition to obtain the average MSD at each lag-time to determine the mechanical properties of the live cells in this experiment.

2.8 Western Blot

2.8.1 Cell harvest and lysate preparation

Cells were harvested by trypsinisation and pelleted by centrifugation at 2000rpm for 2 minutes to remove medium and then washed with sterile 1xPBS. Harvested cells were then lysed by adding lysis buffer (1M Tris-HCL pH6.8, 10% SDS, glycerol, bromophenol blue, β -mercaptoethanol and dH₂O), boiled for 10 minutes and then either used immediately or stored at -20°C prior to electrophoresis.

2.8.2 Sodium dodecyl sulphate-polyacrylamide electrophoresis (SDS-PAGE)

Under denaturing conditions proteins can be separated by their molecular weight in a sodium dodecyl sulphate polyacrylamide gel. Therefore, polyacrylamide gels consisting of a 12% separating gel (1.5M Tris-HCl (pH 8.8), 40% Acrylamide, 10% SDS, 10% APS, TEMED) and a 5% stacking gel (40% Acrylamide, 1.5M Tris-HCl (pH 6.8), 10% SDS, 10% APS, TEMED) were utilised for electrophoresis of protein samples. The polymerization reaction was initiated by adding ammonium persulphate (APS) and TEMED to the separating gel and poured immediately into gel casts. To ensure gels remained moist and air bubbles removed, 1% SDS was applied and the gels were left to set from 10-30min. Once set the 5% stacking gel was applied and left to set. Protein samples were loaded to the gels and gels were placed in a Mini Protean Tetra system (Bio-Rad, USA), submersed in running buffer and electrophoresed at 100 volts until the blue dye present had reached the bottom of the gel. The sample proteins molecular weight was estimated by a protein standard designated "Prestained Protein Marker" was used for comparison. After electrophoresis, proteins were transferred onto nitrocellulose membrane for western blot analysis.

Table 3: Formulations for SDS-PAGE separating and stacking gels.

Reagents	Resolving gel 12%	Stacking gel 5%
H ₂ O	8.6 mL	6.032 mL
40% acrylamide	6 mL	800 µL
1.5M Tris (pH 8.8)	5 mL	-
1.5M Tris (pH 6.8)	-	1 mL
10% SDS	200 µL	80 µL
10% APS	200 µL	80 µL
TEMED	20 µL	8 µL
Total Vol.	20 mL	8 mL

2.8.3 Western blot analysis

Proteins were separated by SDS-PAGE and post electrophoresis gels were transferred onto a nitrocellulose (GE Healthcare, Life science, UK) membrane via a Turbo-blot transfer system (Bio-Rad, USA). Transfers were performed for 1 hour and 30 min at 100volts. Post transfer blots were stained with Ponceau S for 5 minutes, followed by 3 x washes with dH₂O (until background became clear white). Post ponceau staining membranes were washed in 1x PBS-T and blocked for 1 h with blocking buffer. Membranes were then incubated with primary antibodies overnight at 4°C on shaker. Post primary antibody incubation membranes were washed 1 x 10 minutes and 2 x 5 minutes with 1X PBS-T followed by a 1 hour incubation at room temperature with the required horseradish peroxidase (HRP)-linked secondary antibody. Post-secondary antibody incubation, membranes were washed 1 x 10 minutes and 2 x 5 minutes with 1X PBS-T followed by addition of enhanced chemiluminescence (ECL). Bound antibodies were detected by chemiluminescence by exposure to X-ray films. The expression of these proteins were quantified as the densitometry value analysed by ImageJ software and normalised to the appropriate loading control.

Table 4: Primary antibodies used in Western blot.

Antigen	Antibody	MW	Dilution	Source
Actin	Mouse	42 kDa	1:4000	Abcam
β-Tubulin	Mouse	50 kDa	1:5000	Abcam
p38	Rabbit	38 kDa	1:5000	Santa Cruz

2.9 Quantitative Real Time PCR (qRT-PCR)

2.9.1 RNA isolation

To perform qRT-PCR, total RNA was isolated from cultured cells using the High Pure RNA Isolation Kit (Roche Diagnostics, Germany) according to manufacturer's instructions. Cells were suspended in 200µL PBS and 400µL Lysis Buffer. The cell lysate was then transferred to a High Filter Tube, centrifuged for 15sec at 8,000 x g and the flow through was discarded. 90µL DNase Incubator Buffer and 10µL DNase I mix was added and incubated for 15min at 22°C. Next 500µL Wash Buffer I was added and centrifuged for 15sec at 8,000 x g. This step was repeated twice with 500µL Wash Buffer II. The filter tube was transferred to a clean sterile microcentrifuge tube, 50µL Elution Buffer added and centrifuged for 1min at 8,000 x g.

2.9.2 Determination of nucleic acid concentration

The concentration of nucleic acids (RNA) was determined spectrophotometrically using the NanoDrop ND-1000 spectrophotometer (NanoDrop, Wilmington, USA) by measuring absorbance at 260nm and blanked against DEPC water. Pure RNA was estimated by determining absorption ratio A_{260}/A_{280} respectively and stored at -80°C.

2.9.3 cDNA synthesis for RT-PCR

The ImProm-II™ Reverse Transcription System synthesis kit from Promega Corporation (Madison, WI, USA) was used for cDNA synthesis preparation. Initially, the RNA sample was diluted to 5 ng/µL with RNase-free water based on the NanoDrop concentration. RNA sample was incubated for 5min at 70°C in Thermal Cycler PCR machine. According to manufacturer's protocol, 10µL mixture Reverse Transcriptase Kit was added to the diluted RNA sample. The mixture contained 36.6 µL RNase-free water, 24 µL 5x Reaction Buffer, 14.4µL MgCl₂, 6µL dNTP mix, 3 µL RNase, and 6 µL Reverse Transcriptase. The sample was briefly centrifuged

and loaded into the Thermal Cycler PCR machine, programmed as per Table 5: *Settings for Thermal Cycler used for cDNA synthesis*. and the resulting cDNA was stored at -20°C.

Table 5: Settings for Thermal Cycler used for cDNA synthesis.

PCR Step	Temperature °C	Time
Step 1	25°C	5 min
Step 2	42°C	1 hour
Step 3	70°C	15 min
Step 4	4°C	20 min

2.9.4 Synthetic oligonucleotide primers for qRT-PCR

The oligonucleotide primer sequences for all gene products used in qRT-PCR gene expression analysis are listed in table 2.4 below. The oligonucleotides were synthesized by QuantiTect® Primers (Qiagen, UK) and dissolved in 1xTE (Tris-EDTA Buffer) to make up the final concentration.

Table 6: qRT-PCR Primers.

Gene Product	Source	Catalog no.
Human ACTC1	Qiagen	QT00205296
Human TUBB	Qiagen	QT00089775
GUSB	Qiagen	QT00046046

2.9.5 qRT-PCR

Quantitative real time PCR (qRT-PCR) was performed to quantify the changes in gene expression of interest. Reverse transcription was performed as stated in section 2.2.4.3 above. qRT-PCR was conducted using capillaries on an Applied Biosystems StepOne Plus Light Cycler using SYBR Green master mix (Applied Biosystems, CA, USA). The master mix contained 2.6µL RNase-free water, 5 µL 2XKapa, 0.4 µL Primers and 1 µL BSA. Briefly, 1µL of cDNA was combined with the 9µL Master Mix in the capillaries and run on the Light Cycler, programmed as per Table 7 below. Each DNA sample was quantified in duplicate and a negative control without cDNA template was run with every assay to assess the overall specificity. Melting curve analysis was carried out to ensure product specificity. The expression

levels were quantified using the comparative $2^{-\Delta\Delta CT}$ calculation method using GUSB as the housekeeping gene (119).

Table 7: Programme for Light Cycler qRT-PCT machine.

Steps	Temperature °C	Time	Cycles
Denaturation	95°C	3 min	-
PCR	Step 1	95°C	40
	Step 2	55°C	
	Step 3	72°C	
Melting	65°C	15 min	-
Cooling	40°C	30 sec	-

2.10 Data and Statistical Analysis

Raw data for MPTM was collected the confocal microscope and the images processed to obtain quantitative data using ImageJ Fiji. This quantitative data was processed into particle trajectories and further into MSD using Matlab.

Raw data from the Western blot analyses was collected by scanning the photographic films and analysis using ImageJ. Antibody p38 was used for normalization of the data. This data was then statistically analysed.

Raw data from the qRT-PCR method were used to determine the comparative threshold cycle ($\Delta\Delta Ct$)–based fold-change calculations. For these calculations, GUSB was used for normalization of the data. After normalization, the relative expression of each gene was determined for both cell lines (WM1158 and SK-MEL 29). Fold changes in gene expression were expressed as the difference in expression of treated vs untreated cells for both cell lines.

Statistical significance was determined with the student t test for p values less than 0.05. For multiple comparisons, p values were adjusted using Bonferoni correction. Statistical analysis performed using Microsoft Excel and SPSS software version 6.02.

CHAPTER 3: Results

The aim of this study was to identify the effects of chemotherapeutic drug exposure on the mechanical properties and cytoskeletal composition of drug sensitive and drug resistant malignant melanoma cells. A morphology study was initially performed to determine the cytotoxicity of cisplatin and confirm the resistance to the chemotherapeutic drug of the chemoresistant cell line. Multiple particle tracking microrheology (MPTM) was performed to determine the mechanical properties of the cancer cells. Western blot was performed to confirm the presence of the protein product and qRT-PCR was performed for the quantification of gene product of interest.

3.1 Morphology study to assess cytotoxic effect and confirm chemoresistance

Morphology changes between non-treated and treated cells with cisplatin were used to screen for cytotoxic effects of the cisplatin on WM1158 in conjunction with confirming chemoresistance in the SK-MEL 29 malignant melanoma cell line. The cells were treated with a compound concentration that inhibits cell growth by 50% (IC50) for 48 hours. A comparison between WM1158 and SK-MEL 29 cell lines were made by imaging the cells at 0 hours, 24 hours and 48 hours, to determine the effect of the chemotherapeutic treatment over time and presence of chemoresistance.

In Figure 10a and b it is evident that at 0 hours cells are replicating, as mitosis is occurring expressed by the white halo surrounding the cells. Comparing the 24 hours post treatment time point (Figure 10c) expresses the rounds of cells with no mitosis and (Figure 10d) reveals that cells maintained morphological structure and presences of mitosis. The 48 hour post treatment time point revealed (Figure 10e) complete rounding of cells as an indication of apoptosis compared to (Figure 10f) expressing normal morphological patterns and presence of mitosis still present.

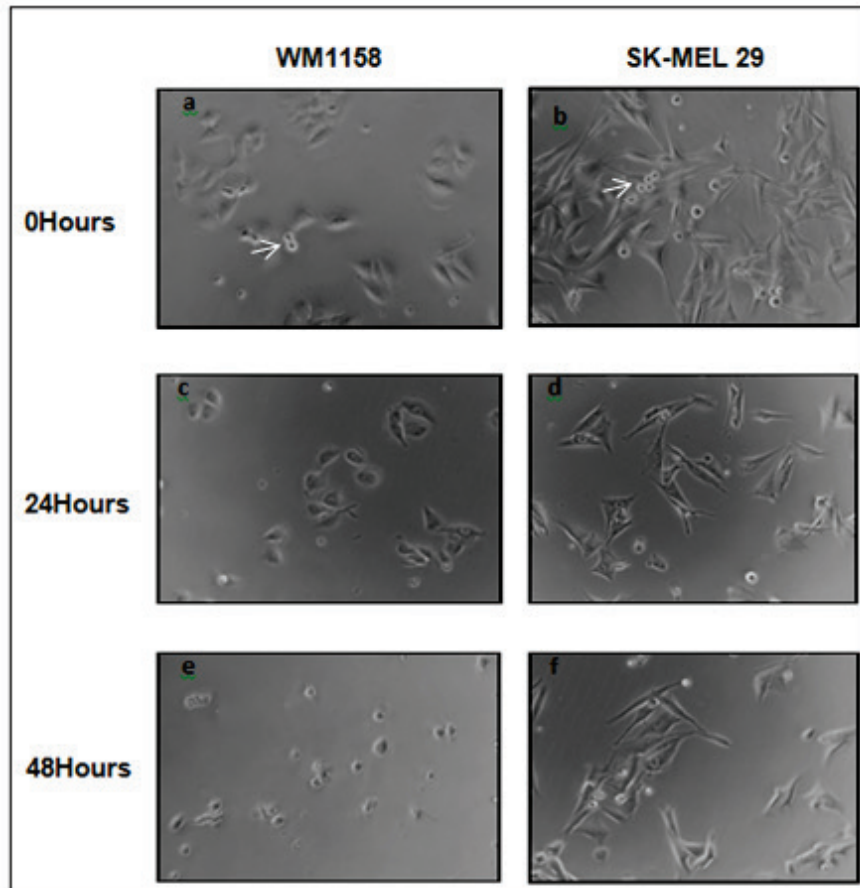


Figure 10: Cisplatin cytotoxic effects on WM1158 and presence of chemoresistance in SK-MEL 29. Representative phase-contrast photomicrographs (400x; Olympus 1X71) showing WM1158 and SK-MEL 29 cells treated with Cisplatin at 0 hours (**a, b**), Cisplatin treatment at 24 hours (**c, d**), and Cisplatin treatment at 48 hours (**e, f**), inserted arrows (a, b) indicating white halo of cells undergoing mitosis.

3.2 Cell mechanical properties obtained by multiple particle tracking microrheology

Multiple particle tracking microrheology (MPTM) was performed to probe the mechanical properties of individual living cells and the MSD of MitoTracker-stained mitochondria embedded in the cells was then calculated. The MSD provides information concerning the motion of particles in cytoplasm and indirectly about the cell microenvironment mechanics.

The MSD of non-chemoresistant malignant melanoma cell line WM1158 was compared to the chemoresistant malignant melanoma cell line SK-MEL29. Both cell lines were then treated with cisplatin for 24 hours and then exposed to the MitoTracker prior to MPT as mentioned in objective 3.

3.2.1 Non-resistant Cancer Cells without Treatment

MPTM was used as it determines the mechanical properties of WM1158 cancer cells, i.e. locally measures the viscoelastic properties of the cytoplasm. Cells were cultured and exposed to MitoTracker 30 min before microscopy. Under a 60X (oil immersion) objective lens on the confocal microscope, the fluorescent MitoTracker-stained mitochondria were visible inside the cells, which was explained in detail in section 2.2.6.1. The mechanical properties of WM1158 malignant melanoma cells were determined by capturing a time series images of single cells at 0.05fps for the duration of 90sec.

Figure 11a shows an example of overlay image of a single cell exposed to MitoTracker during the monitoring process of the time series. Figure 11b shows the example of particle trajectories expressing Brownian motion of the cell in Figure 11a.

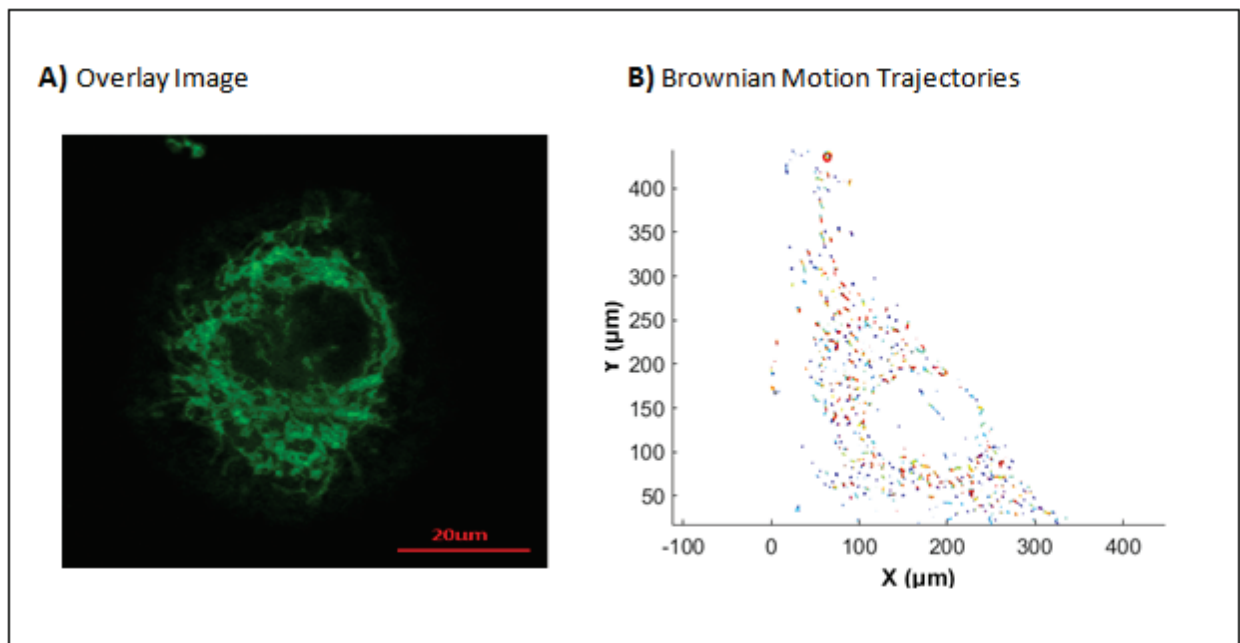


Figure 11: Particle Trajectories of WM1158 cancer cells. a) Fluorescence micrograph used for the identification and tracking of particles within the cell, with scale bar representing 20 μm. b) Visualisation of imported trajectories expressing Brownian motion.

3.2.2 Chemoresistant cancer cells without treatment

The mechanical properties of SK-MEL29 chemoresistant malignant melanoma cells were determined by capturing a time series images of single cells at 0.05 frames per second (fps) for the duration of 90sec.

Figure 12a shows an example of overlay image of a single cell exposed to MitoTracker during the monitoring process of the time series. The cell displayed extensive expression of MitoTracker which was distributed relatively heterogeneously throughout the cell as detected by fluorescent microscopy. Figure 12b shows the example of particle trajectories expressing Brownian motion of the cell in Figure 12a.

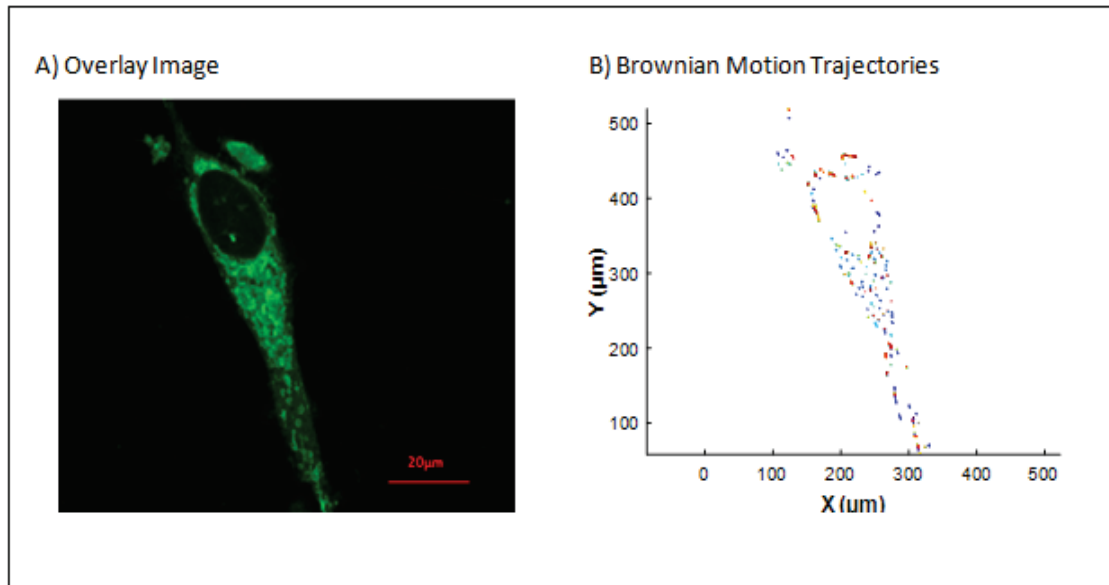


Figure 12: Particle Trajectories of SK-MEL29 cancer cells. a) Fluorescence micrograph used for the identification and tracking of particles within the cell, with scale bar representing 20 μm . b) Visualisation of imported trajectories expressing Brownian motion.

3.2.3 Non-resistant and chemoresistant cancer cells exposed to chemotherapeutic drugs

Both WM1158 and SK-MEL29 cell lines were treated with cisplatin 24 hours before exposure to the MitoTracker. Figure 13 shows the effects of cisplatin on the cells exposed to the MitoTracker and DMSO as a positive result for both WM1158 and SK-MEL29 as a comparison.

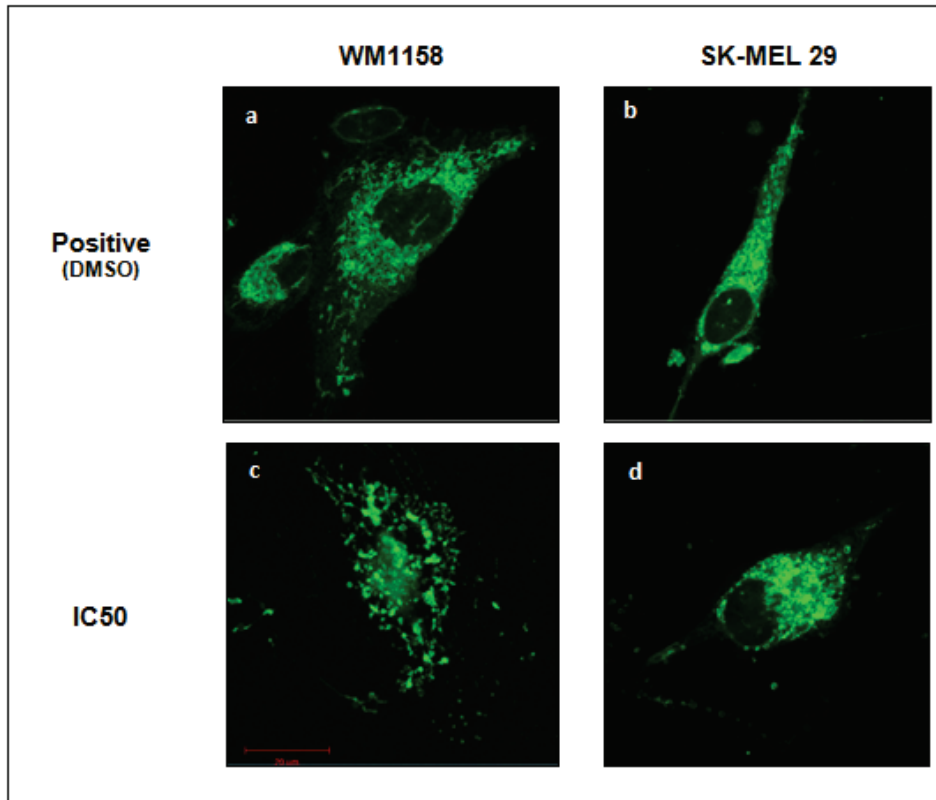


Figure 13: Cisplatin treated cells exposed to mitotracker for determination of mechanical properties of cancer cells. Representative confocal photomicrographs showing WM1158 and SK-MEL 29 cells with positive controls with mitotracker and no treatment (**a, b**), and Cisplatin treated with concentration IC50 and mitotracker (**c, d**). Images were captured under a confocal microscope (Zeiss, Germany) at 600x magnification and are representative of a randomly selected field for each condition (scale bars indicate 20 μ m).

As seen in Figure 13c the cisplatin and MitoTracker combined was too harsh for WM1158 cell line and caused all cells to undergo apoptosis. This experiment was repeated 3x times, producing the same results in all instances. The mechanical property expression could therefore only be determined on SK-MEL29 chemoresistant malignant melanoma cell line. Figure 14a shows an example of an overlay image of a single cell exposed to cisplatin and MitoTracker during the monitoring process of the time series. The cell displayed extensive expression of MitoTracker which was distributed relatively heterogeneously throughout the cell as detected by fluorescent microscopy. Figure 14b shows the example of particle trajectories expressing Brownian motion of the cell in Figure 14a.

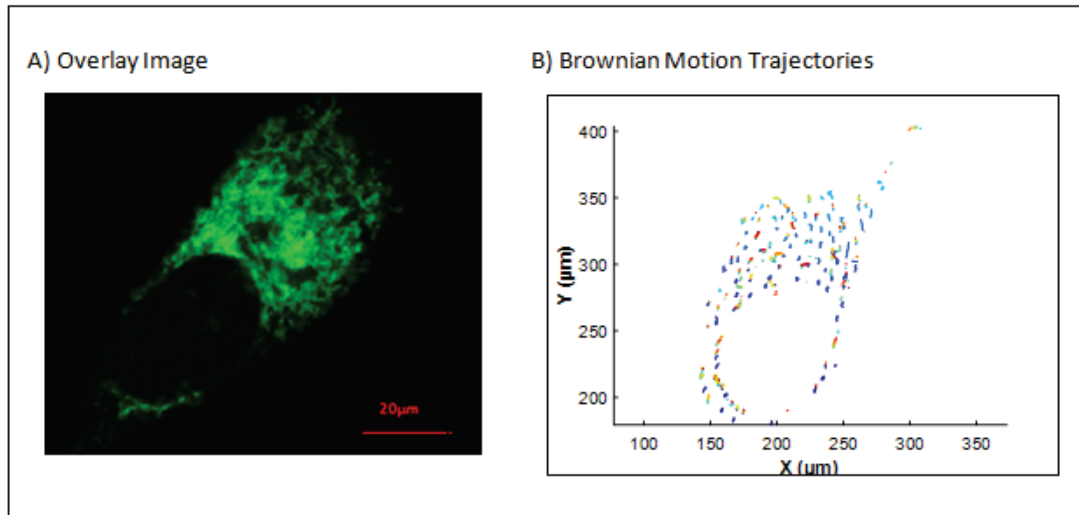


Figure 14: Particle Trajectories of SK-MEL29 cancer cells exposed to cisplatin. A) Fluorescence micrograph used for the identification and tracking of particles within the cell, with scale bar representing 20 μm . B) Visualisation of imported trajectories expressing Brownian motion.

3.2.4 Cancer cell mechanics presented as MSD values

After imaging, the particles were tracked in the time laps images using MATLAB tracking software as described in section 2.2.6.2 and the MSD was computed. Figure 15 shows the graph of ensemble MSD vs lag time in for WM1158 cells and SK-MEL29 cells studied in this experiment. The graph illustrates that the slope of MSD vs τ is $0 < \alpha < 1$, indicating a sub-diffusion dynamic behaviour for the motions of the intracellular particles in the studied cancer cell lines over time intervals.

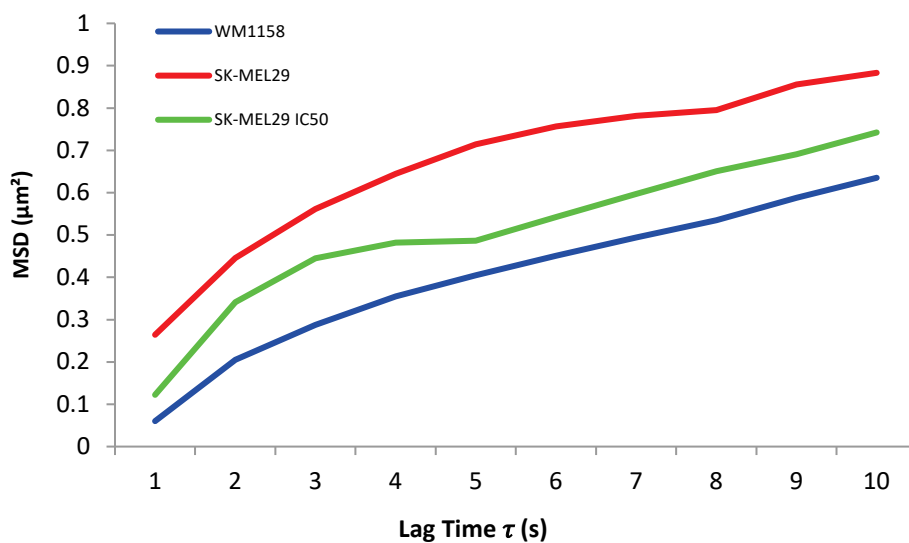


Figure 15: Cancer cell mechanics presented as MSD over lag time. A diagram of the ensemble averaged MSD vs lag time for cell lines WM1158, SK-MEL29, and SK-MEL29 IC50 exposed to cisplatin.

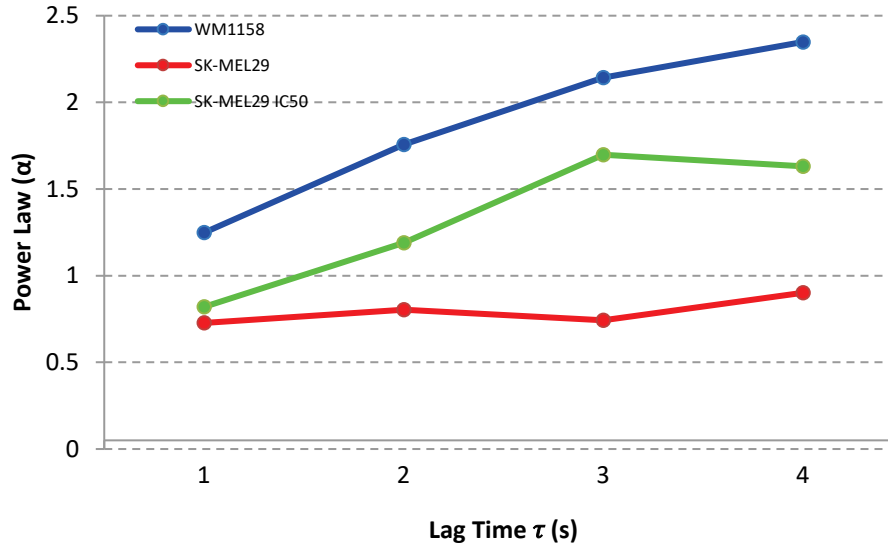


Figure 16: Power Law coefficient α obtained from MSD values. A diagram portraying the α values of both WM1158 and SK-MEL29 cell lines under the two conditions of Mitotracker exposure only and Mitotracker combined with cisplatin treatment. The MSDs of particle trajectories from the Mitotracker anchored to the mitochondria within cancer cells which exhibits anomalous diffusion dynamics as presented in equation 2 from section 1.3.3.2, $\langle \Delta r^2(t) \rangle \sim t^\alpha$ (subdiffusive $\alpha < 1$ and superdiffusive $\alpha > 1$).

As shown in Figure 16, the WM1158 cell line exhibited a super-diffusive pattern with mean $\alpha=1.99$ for a lag time of up to 4 s. The SK-MEL29 chemoresistant malignant melanoma cell line presented a pure diffusion dynamic behaviour with mean $\alpha=0.86$, i.e. ≈ 1 for the motions of the intracellular particles throughout time intervals. Lastly, the SK-MEL29 IC50 condition revealed sub-diffusion dynamic behaviour (mean $\alpha=1.46$) for the motions of the intracellular particles at short time intervals.

3.3 Molecular adaption of the cytoskeletal properties of malignant melanoma cells assessed by Western Blot

3.3.1 Actin protein expression

The protein expression of actin was determined in both cell lines by SDS-Page and immunodetection. Briefly, cell lysates were prepared from 70-80% confluent cells and loaded onto polyacrylamide gels as described in section 2.2.3. Actin was resolved on precast SDS12% gels. Following electrophoresis, proteins were electrotransferred onto nitrocellulose and probed for target protein using specific antibody (Table 4). A monoclonal antibody commercialised by Life Technologies was utilised, with p38 as a loading control. The predicted molecular weight of actin is 42kDa (Figure 17).

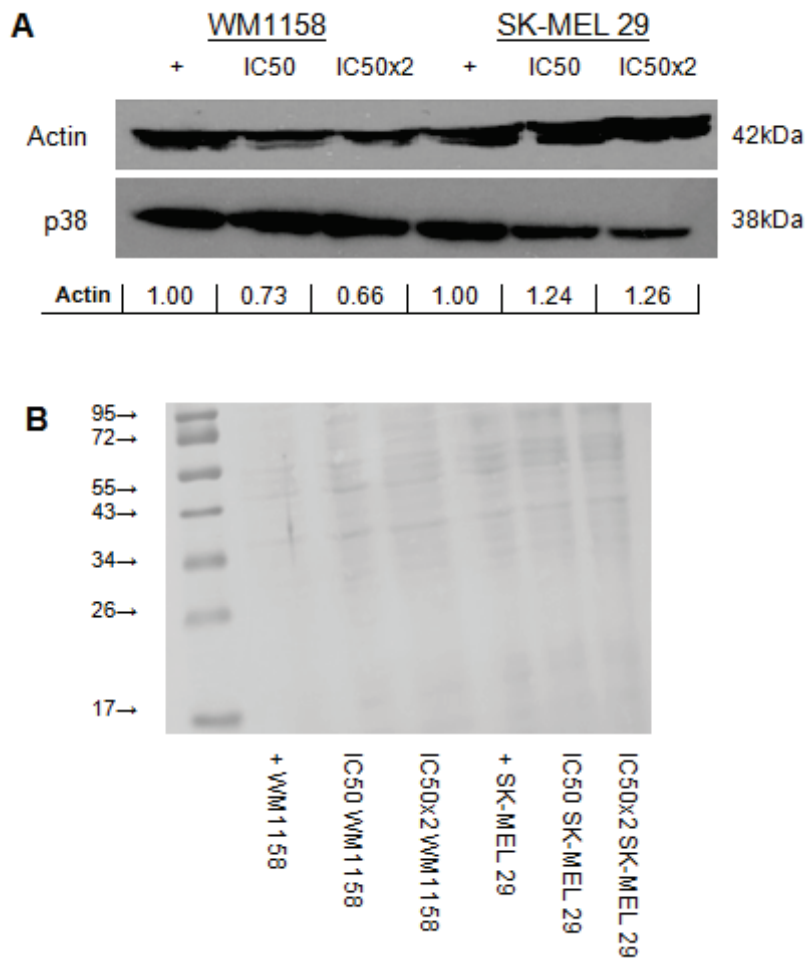


Figure 17: Actin protein analysis. A) Western Blotting of cell extracts from WM1158 and SK-MEL29 visualising actin protein indicated at approximately 42 kDa and normalised to corresponding p38 signals. The conditions for this experiment represent positive (+) as no treatment, IC50 as half the inhibitory concentration dose of cisplatin and 2xIC50 as twice the inhibitory concentration dose of cisplatin. Image J image analysis software was used to quantify signal intensities; these signal intensities are shown in the table below the western blot. **B)** Successful transfer of proteins onto the membrane and visualized by ponceau stain, serving as normalization for protein loading.

It is evident that there is a decrease in actin protein in the treated conditions, i.e. IC50 and 2xIC50, compared to the non-treated condition of the WM1158 cell line. In contrast to the non-resistant WM1158 cell line, the chemoresistant SK-MEL29 cell line exhibited increased actin levels for treatment conditions compared to the non-treated condition. Quantification of protein expression is shown in Figure 18.

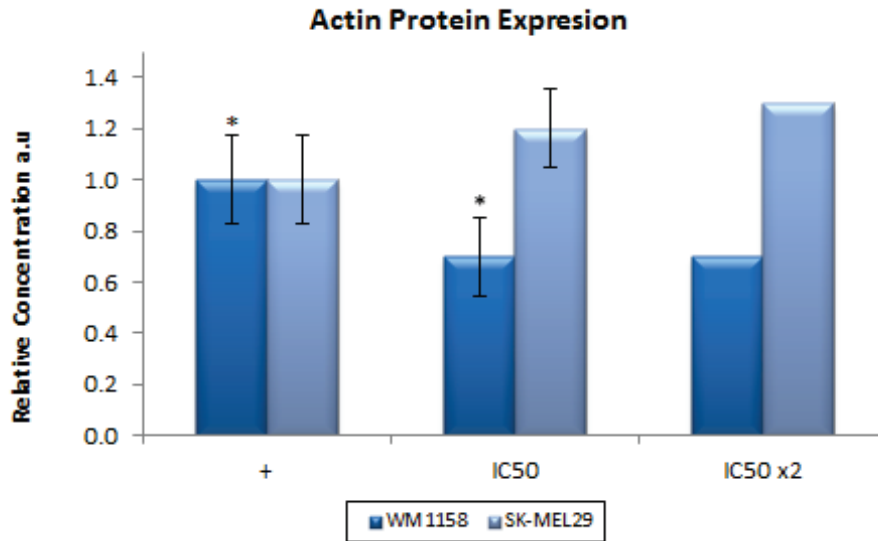


Figure 18: Quantification of Actin protein expression. Histogram representing the expressing of relative actin protein concentrations (fold change) throughout the various experimental conditions obtained from Western blot quantification via ImageJ. The conditions for this experiment represent positive (+) as no treatment, IC50 as half the inhibitory concentration dose of cisplatin and 2xIC50 as twice the inhibitory concentration dose of cisplatin, with error bars representing the STDEV. Asterisks indicated statistical significance of treated conditions compared to the non-treated control of the same cell line.

3.3.2 β -Tubulin protein expression

The protein expression of β -Tubulin was determined in both cell lines by SDS-Page and immunodetection. Briefly, cell lysates were prepared from 70-80% confluent cells and loaded onto polyacrylamide gels as described in section 2.3.3. β -Tubulin was resolved on precast SDS12% gels. Following electrophoresis, proteins were electrotransferred onto nitrocellulose and probed for target protein using specific antibody (Table 4). A monoclonal antibody commercialised by Life Technologies was utilised, with p38 as a loading control. The predicted molecular weight of β -Tubulin is 50kDa (Figure 19).

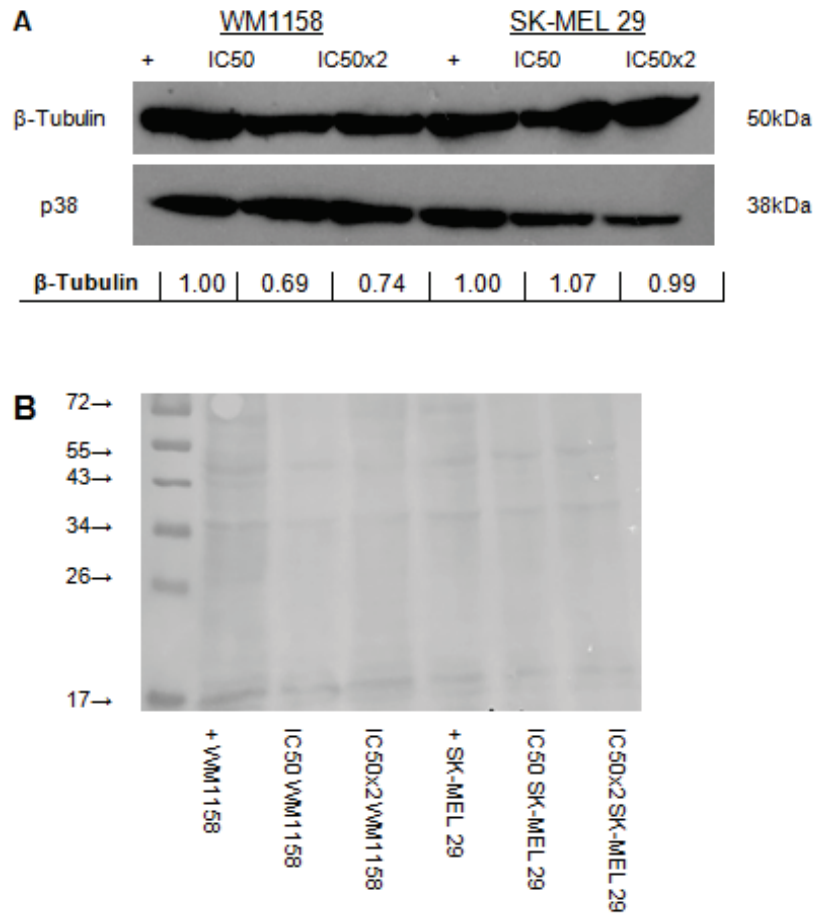


Figure 19: β -Tubulin protein analysis. a) Western Blotting of cell extracts from WM1158 and SK-MEL29 visualising actin protein indicated at approximately 50 kDa and normalised to corresponding p38 signals. The conditions for this experiment represent positive (+) as no treatment, IC50 as half the inhibitory concentration dose of cisplatin and 2xIC50 as twice the inhibitory concentration dose of cisplatin. Image J image analysis software was used to quantify signal intensities; these signal intensities are shown in the table below the western blot. b) Successful transfer of proteins onto the membrane and visualized by ponceau stain, serving as normalization for protein loading.

With regards to β -Tubulin it is evident that there is a similar protein expression pattern as seen in actin protein expression. For the WM1158 cell line, β -tubulin decreases in IC50 and IC50x2 treatment conditions compared to non-treated control. The chemoresistant SK-MEL29 cell line shows, however, an increase in protein expression for IC50 treatment condition and no change for the IC50x2 treatment compared to the non-treated control. Quantification of protein expression is shown in Figure 20.

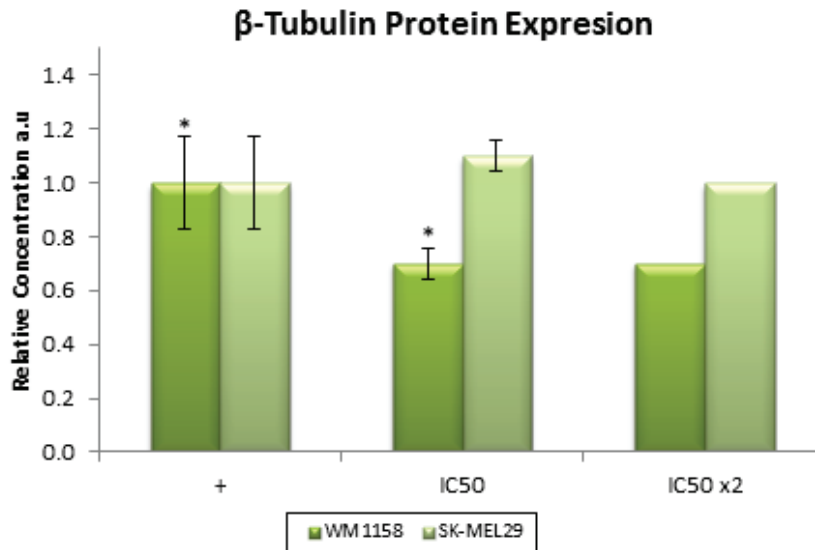


Figure 20: Quantification of β-Tubulin protein expression. Histogram representing the expression of relative β-Tubulin protein concentrations throughout the various experimental conditions obtained from western blot quantification via ImageJ. The conditions for this experiment represent positive (+) as no treatment, IC50 as half the inhibitory concentration dose of cisplatin and 2xIC50 as twice the inhibitory concentration dose of cisplatin, with error bars representing the STDEV.

3.4 Gene expression of cytoskeletal properties of malignant melanoma cells assessed by qRT-PCR method

3.4.1 Actin mRNA expression

After confirming a decreased expression of actin protein in WM1158 treated cells, mRNA expression was determined by qRT-PCR as described in section 2.2.4. Relative expression were calculated for both cell lines and compared to their respective control cell lines. The mRNA expression of housekeeping gene GUSB (primer details in Table 6) was used to standardise the samples. The relative expression of ACTC1 mRNA was calculated as the ratio between the expression of ACTC1 gene and the expression of the housekeeping gene, with a negative control included in each experiment.

Figure 21 shows the data from this experiment, which demonstrated low mRNA expression of the ACTC1 in WM1158 cells compared to SK-MEL29 (relative mean expression = 4.18, $p < 0.005$).

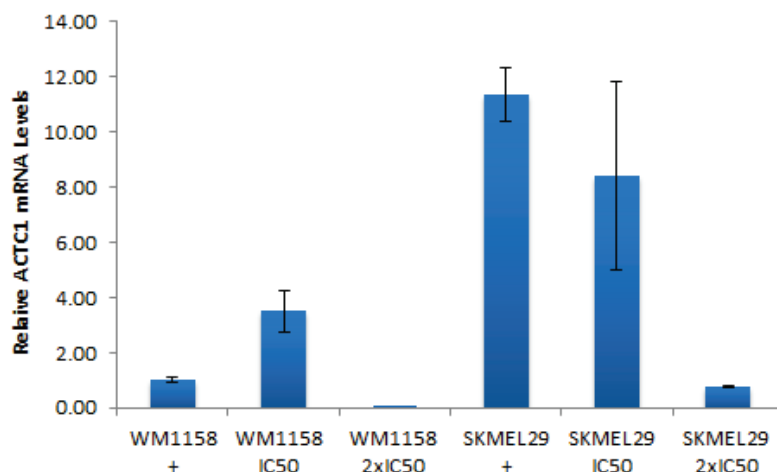


Figure 21: qRT-PCR estimated mRNA concentration. Bar graph illustrating the relative normalised mRNA concentration for WM1158 and SK-MEL 9 cell lines. Primers specific to actin (ACTC1) was used and in both indicated cell lines, mRNA levels were first normalised to GUSB and then expressed relative to actin. The conditions for this experiment represent positive (+) as DMSO only no cisplatin treatment, IC50 as half the inhibitory concentration dose of cisplatin and 2xIC50 as twice the inhibitory concentration dose of cisplatin, with error bars representing the STDEV.

3.4.2 β -Tubulin mRNA expression

After confirming a decreased expression of β -Tubulin protein in WM1158 treated cells, mRNA expression was determined by qRT-PCR as described in section 2.2.4. Relative expression was calculated for both cell lines and compared to their respective control cell lines. The mRNA expression of housekeeping gene GUSB (primer details in Table 6) was used to standardise the samples. The relative expression of TUBB mRNA was calculated as the ratio between the expression of TUBB gene and the expression of the housekeeping gene, with a negative control included in each experiment.

Figure 22A shows the data from this experiment, which demonstrated a decreased mRNA expression of the TUBB in WM1158 treated cells compared the untreated WM1158 cells and SK-MEL29 cells (relative mean expression = 0.79, $p < 0.66$).

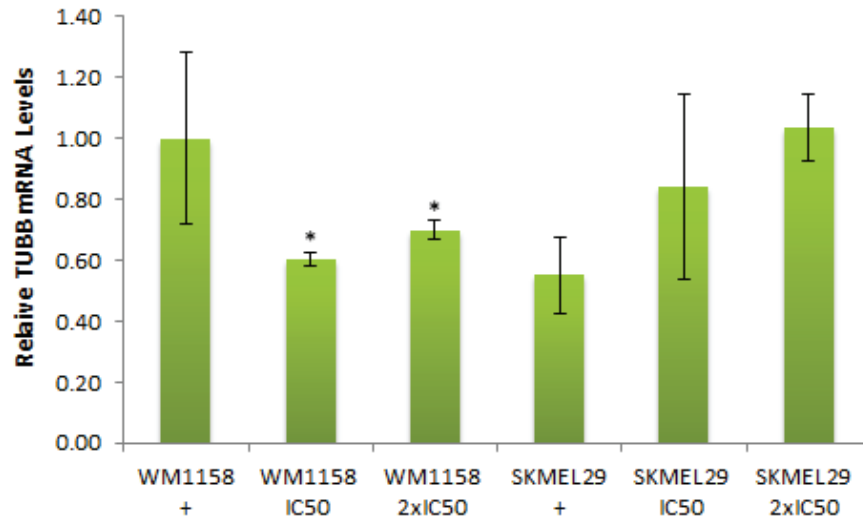


Figure 22: qRT-PCR estimated mRNA concentrations. Bar graph illustrating the relative normalised mRNA concentration for WM1158 and SK-MEL 9 cell lines. Primers specific to β -Tubulin (TUBB) was used and in both indicated cell lines, mRNA levels were first normalised to GUSB and then expressed relative to β -Tubulin. The conditions for this experiment represent positive (+) as DMSO only no cisplatin treatment, IC50 as half the inhibitory concentration dose of cisplatin and 2xIC50 as twice the inhibitory concentration dose of cisplatin, with error bars representing the STDEV.

CHAPTER 4: Discussion

Cancer patients treated with chemotherapeutic agents usually show a promising initial response, however patients that relapse ultimately succumb to their disease due to the development of resistance (120). Regulation of cellular drug uptake, increased DNA damage repair, and inhibition of apoptosis have been proposed to cause chemoresistance (121). The development of strategies for chemosensitization and prevention of therapeutic resistance remains a major goal with important clinical implications.

Cellular mechanical properties serve as a powerful label-free marker that could be used to gain insight into changes on a molecular scale within the cell. It is also useful in characterising different cellular stages and states for the use of potential diagnostic information. Most cancer forms have a long latency period causing the diagnosis to only take place at late stages of the disease; at this stage unfortunately resistance to chemotherapy is already present. For these reasons mentioned and the fact that chemoresistance is not easily detectable, identification of new and specific biomarkers is critical in guaranteeing early detection and defining treatments that would be more efficient (122-124). This is evident that during cancer progression a cell progresses from a full mature post mitotic state cell to a motile proliferative cancerous state. During this process, dramatic reorganisation of the actin cytoskeleton occurs that lead to a deviation from the original mechanical properties of the cell (125, 126).

In this study, the mechanical properties of non-resistant and chemoresistant cancer cells were studied in malignant melanoma cells to determine the mechanistic basis for chemoresistance. These cells were chosen based on their aggressive nature. Malignant melanoma is an aggressive skin cancer with its incidence rate worldwide increasing faster than any other known cancer type (127). The survival rate is presently less than 10% and patients having a 10-year survival rate upon being diagnosed with metastatic melanoma (128). However surgery being a successful treatment for primary melanomas, treatment options for metastatic melanoma remains to be a change and is mainly treated with chemotherapeutic drugs. Metastatic melanoma however is reported to be the most resistant to chemotherapeutic drugs of all human cancers and based on this fact has been chosen as cells of choice for this study (129).

As noted in chapter 1, the organisation of specific cytoskeletal elements such as actin and tubulin can reflect the diverse mechanical properties of the cells of interest. To date, there has been little characterisation of these two major cytoskeletal elements composition (130, 131) and none that directly compared the cytoskeletal composition of malignant melanoma and chemoresistance. Therefore, in this study we have utilised a combination of scanning laser

confocal microscopy coupled with the multiple particle tracking microrheology, quantitative RT-PCR and Western blotting to analyse the organisation of and quantify actin and β -tubulin in malignant melanoma and resistant malignant melanoma cell lines.

4.1 Morphological Examination

The overall morphological appearance was studied to determine the cytotoxic effect of cisplatin on non-resistant malignant melanoma cells WM1158 and to confirm the resistance of chemoresistant malignant melanoma SK-MEL29 cells. WM1158 and SK-MEL29 cells were exposed to an IC50 concentration of cisplatin for 48 hours. The cells' morphology was observed at three time points (0 hours, 24 hours and 48 hours). Distinct differences in cellular morphology were observed by bright field light microscopy (Figure 10) between the metastatic melanoma cell line WM1158 and the resistant metastatic melanoma cell line SK-MEL29.

Compared to 0 hour exposure, cisplatin displayed a potent cytotoxic activity in the WM1158 cells at 48 hours. Cell line SK-MEL29 however displayed no change to the cisplatin exposure and continued proliferation. At 24 hours, cell line WM1158 displayed an epithelial cell like shape while the resistant SK-MEL29 cells displayed spindle-shape morphology in response to the cisplatin treatment. Based on these results it is evident that the cisplatin utilised in this study had strong cytotoxicity levels and that SK-MEL29 was indeed chemoresistant.

4.2 Multiple Particle Tracking Microrheology

In this study, a new functional microscopy technique, MPTM, has been employed which allows the local micromechanics of living cells to be probed. This technique allows for the measurement of averaged cell parameters to be compared to parameters obtained from more classical approaches and allows spatial variations of intracellular mechanics to be revealed. Previous works have made use of classical approaches by either studying mechanical properties without the control of cell geometry thereby on focusing on large cell-to-cell viability (80, 132, 133) or by using a more conventional approach of atomic force microscopy or magnetic twisting cytometry that measures the cells surface regional rigidity variations (134-136).

Central to this approach is the statistical analysis of the MSD of particle trajectory distributions throughout the cells' cytoplasm making use of Brownian motion and the power law. In this study we evaluated the mechanical properties of malignant melanoma WM1158 and chemoresistant malignant melanoma SK-MEL29 cells, measuring MSDs of tracked particles

attached to the intracellular mitochondria using MPTM. Previous work have found that MSD amplitude is shown to be inversely related to intracellular stiffness (137), based on this principle the MPTM experiment was performed.

The time-lapse imaging of the mitochondria in the cytoplasm allowed for direct mapping of the displacement field of the malignant cell's cytoplasmic environment, which can be seen in Figure 11, Figure 12 and Figure 14, respectively. From these images the particle trajectories were presented expressing Brownian motion. Microrheology measures this Brownian motion and relates this motion into rheological properties, such as viscosity, using the generalised Stokes-Einstein relation (GSER) as described in section 1.3.3.2. According to the power law exponent (α) (equation 2) is a representative of the type of motion the particle undergoes. This state of the particles within the cell of interest can be determined using the logarithmic slope of MSD which is determined at the shortest lag times measured by MPTM. The shortest lag times are the largest frequencies measured and thereby capture the longest relaxation times of the particles. With regards to cisplatin treated WM1158 cells it had been found that the treatment in combination with the MitoTracker was an extreme harsh environment and causing cells to undergo apoptosis as seen Figure 13.

The individual mitochondrial MSDs of each cell has great variability in the distribution of the slope, this is due to individual cells being extremely heterogeneous and so each particle will express a different MSD depending on its location within the cell. Based on this principle, the ensemble average MSDs obtained from all cells of each cell line and experimental condition were plotted. As shown in Figure 15, the ensemble average of MSD of WM1158 cells clearly shows an increase in the slope of the MSD curve with an increased lag time indicating a super-diffusive motion behaviour at particular time intervals associated with a loss of stiffness and decrease in elastic nature of the cells. A similar trend was observed in SK-MEL29 exposed to treatment shown in Figure 16. For the chemoresistance cell line SK-MEL 29 with no treatment, the ensemble averaged MSDs show an increase in amplitude with $\alpha = 1$ representing a pure diffusion of fluid-like motion (Figure 16).

This MPTM study revealed changes in the internal mechanism and activity of cells exposed to chemotherapeutic agents and cells undergoing transformation. The results from this study showed that MSDs in SK-MEL29 cells without drug exposure were significantly higher than those in WM1158 and SK-MEL29 treated cells; this is due to cells being less dense and possessing a more active cytoskeletal network. These results suggest that tumorigenicity of cells largely correlated with an increase in intracellular activity and a decrease in cell stiffness and structural density. Based on these results and measurement of mechanics over time, it is also suggested that apoptosis causes cells to become more viscous and elastic over time.

From the findings from the MPTM experiment, we propose that, in the case of malignant tumours, cellular stiffness was drastically reduced i.e. cells were softer nature in non-resistant malignant cell line than the chemoresistant cell line. Comparing non-resistant cells to chemoresistance cells, the resistant SK-MEL29 cells proved to have less elasticity and be stiffer in nature.

4.3 Western blot analysis

A protein expression study was conducted by means of Western blotting. Sample blots were analysed quantitatively, normalised to p38 and compared to untreated cells which also functioned as a control for statistical difference determination. Protein levels of actin and β -tubulin were quantified and altered expression levels of both cytoskeletal elements were found comparing WM1158 to resistant SK-MEL29 cell line (Figure 17a & Figure 19a, respectively). The results highlighted the presence of actin at approximate 42 kDa and β -tubulin at approximately 50 kDa that matches the predicted size as per antibody datasheet.

Actin is found to be the most abundant protein in eukaryotic cells. Due to its highly conserved nature it participates in more protein-protein interactions than any other known protein. Actin also has the ability to transition between monomeric (G-actin) and filamentous (F-actin) states under the control of ions, nucleotide hydrolysis and a number of actin-binding proteins (138). These transitional abilities along with the mentioned properties make actin a critical part in many cellular functions. These functions range from cell motility to the maintenance of cell shape and polarity of transcription regulation. Based on this, the expression of actin was used to evaluate the protein expression in cancer cells and chemoresistant cells in conjunction with mechanical evaluations. The expression of actin protein levels in WM1158 cells revealed a significant down regulation in treated cells compared to untreated (control) cells. Nevertheless, SK-MEL29 cells presented with an up-regulated protein expression when comparing treated to untreated (control) cells (Figure 18).

β -Tubulin is a heterodimer found in the dynamic intracellular structure known as the microtubule cytoskeleton. The microtubule cytoskeleton plays a critical role in supporting cellular structure; transporting vesicles, proteins, and organelles; and enabling cell motility. Due to the nature of β -Tubulin and its important role in the cytoskeleton of cells it was used to evaluate the protein expression in cancer cells and chemoresistant cells in conjunction with mechanical evaluations. With regards to β -tubulin, a similar pattern as for actin protein can be seen in both WM1158 and SK-MEL29 cell lines for both treated and untreated conditions

(Figure 20). These results indicated that cisplatin produced a difference in the amount of protein expression in the treated cells compared to the control.

Studies have found that platinum compounds such as cisplatin are able to bind to cellular proteins of the cytoskeleton such as actin and tubulin (139, 140). Consistent with this, the current study revealed that cisplatin treatment of the non-resistant WM1158 cell line clearly affects the cytoskeleton by causing morphological changes as well as distinct changes in the protein expression of actin and β -tubulin. Cytoskeletal changes observed for treatment of chemoresistant cells were not statistically significant, and the slight up regulation of protein levels is ascribed largely to the continuous differentiation of malignant tumour progression.

4.4 qRT-PCR analysis

Quantitative RT-CPR was conducted to analyse the mRNA expression for both actin and β -tubulin to determine if any inherent gene differences were present leading to cytoskeletal element changes in the presence and absence of cisplatin. The mRNA expression of actin (ACTC1) and β -tubulin (TUBB) for both WM1158 and SK-MEL29 cells were normalised to GUSB a housekeeping gene and compared to untreated cells which also functioned as a control for statistical difference determination.

In addition to the effects of cisplatin presented at the protein level, we demonstrated a differential gene regulation at the mRNA level. The relative actin mRNA levels were affected in a similar manner to the protein expression in WM1158 and SK-MEL29 cells (Figure 21), suggesting that cisplatin's point of interference was the DNA sequence. However, β -tubulin mRNA and protein expression was influenced differently by cisplatin treatment, with a decrease in protein expression (as mentioned in section 4.3), but an increase in mRNA expression (Figure 22). This pattern had been found in previous studies and suggests that cisplatin may influence certain genes differently at the post-transcriptional or post-translational levels without affecting the DNA sequence, which could be linked to epigenetic regulation (141, 142).

It has been found that at IC50 dose of cisplatin, the chemotherapeutic drug kills tumour cells by interfering with the cellular structure and function at the DNA level, which is also evident in this study. At the same time as cellular structure and DNA function are affected, cisplatin appeared to regulate gene expression, and therefore to interfere with the stage of cellular differentiation, both at the mRNA and protein levels. This is in agreement with previous studies showing that some tumour cells require high doses of chemotherapeutic agents to undergo complete apoptosis (143-145). Low, non-toxic dosage may however have a different effect on

the cells without causing cell death. This differential response suggests that cisplatin may act in tumour-specific manner, depending on the properties and cellular hierarchy manifested by each tumour. Based on these findings it has been found that development of chemoresistance depends largely on the type of tumour, its progression and dosage and exposure time of the chemotherapeutic drug.

4.5 Overall Findings

Using a combination of Multiple Particle Tracking Microrheology, quantitative RT-PCR and Western blotting, we have demonstrated that actin and β -tubulin have altered architectures as well as differences in protein and gene levels in malignant melanoma cells and chemoresistant malignant melanoma cells. We have applied intracellular MPTM in live cells to study the mechanical properties of malignant cancer cells and cancer cells exposed to chemotherapeutic drugs. Using MPTM we were able to detect and provide quantitative estimates of cellular mechanical property changes that occurred in each condition. It was shown that cell stiffness decreases as the cancer cells' metastatic potential increases; thereby as cancer progresses the cells become stiffer. This pattern was evident for chemoresistant malignant cells as well and revealed that they had a loss of elasticity in comparison to their counter non-resistant malignant cells. With regards to protein levels and mRNA expression, cisplatin affected the cytoskeleton causing cells to undergo morphological changes which, however, was not seen in chemoresistant cells. These findings suggest in particular that chemoresistance development depends largely on the type of cancer and its stage of progression and also the chemotherapeutic agent dosage and exposure times.

CHAPTER 5: Conclusion

This study is one of the first investigations that makes use of a combination of bioengineering and molecular approaches to compare the response of drug-sensitive and drug-resistant malignant melanoma cells to chemotherapeutic drug exposure. The findings from this study and MPTM experiments identified biophysical cell parameters for the screening of cancer and its progression. We hypothesised that exposure to a chemotherapeutic drug leads to a change in intracellular stiffness of malignant melanoma cells and found that malignant chemoresistant cells are indeed stiffer in nature. In particular, this study revealed that single cell mechanical phenotyping appears to be a quick and efficient marker and additional support in cancer diagnosis providing a deeper understanding of cancer mechanobiology and in the definition of new diagnostic tools for chemoresistance in cancer therapies.

5.1 Future Research

MPTM has been found to be a useful tool in studying the mechanical properties of live cells. In this work, by staining, the mitochondria were used as tracker particles that enter the cells by endocytosis and attached to the mitochondria within the cytoplasm. A limitation experienced in this study was the harsh apoptotic effects that the Mitotracker combined with cisplatin treatment had on the non-resistant cell line. This could largely be due to the means by which the Mitotracker enters the cells and the incubation time of exposure before viewing using confocal microscopy. Future studies could possibly address this issue by either exploring different incubation times of Mitotracker exposure with different dilution concentrations. The Mitotracker dilution concentration could be adjusted in combination with different exposure times to determine the optimal concentration of Mitotracker combined with chemotherapeutic drug. By finding an optimal dilution concentration it may be possible to limit the cytotoxicity of the Mitotracker combined with cisplatin and allow the cell wall to undergo some form of repair with a longer incubation period. However, it should be noted that the aim of cisplatin is indeed to cause cells to undergo apoptosis and thereby provides limited incubation time before cytotoxicity levels are reached.

There are however other methods for the insertion of particle tracers into cells. An interesting aspect could be to compare the results obtained from various methods, such as microinjection and ballistic injection. Using these methods might allow a less harsh environment for treated non-resistance cells allowing the full scope of the study. The ballistic method is interesting in particular that it allows for much larger tracking environment with less damage to cells with

respect to the microinjection (146). By using different types of particles and injection methods a more complete picture of the cell's mechanical properties can be obtained. These methods would also allow for the measurement of how the cellular properties change in different locations within the cell such as the nucleus compared to the cytoplasm. This will develop a mechanical map that will part of the cell is predominantly responsible for the chemoresistance development. A mechanical mapping of a cell could be developed at different time points for both treated and un-treated cells. This would however require a mathematical tool such as the tools developed for non-biological materials to be developed (147). These methods propose an advantage to the scope of the study, nevertheless they are each presented with their own limitations that might affect the study in a different dynamic and may alter the end result in some form.

REFERENCES

1. Society: AC. American Cancer Society: Cancer Facts & Figures. Atlanta 2013. p. 1-60.
2. Cheung-Ong K GG, and Nislow C. DNA-Damaging Agents in Cancer Chemotherapy: Serendipity and Chemical Biology. *Chem Biol.* 2013;20:648-59.
3. Fidler F. and Soerjomataram I. The global cancer burden and human development: A review. *Scandinavian Journal of Public Health.* 2017;46(1):1-20.
4. American Cancer Society. Cancer Treatment & Survivorship Facts & Figures 2016-2017. Atlanta: American Cancer Society; 2017. Available: <https://www.cancer.org/research/cancer-facts-statistics/survivor-facts-figures.html> [2016, May 9].
5. Hassan AJ, Spooner D, and Hussain SA. Chemotherapy for breast cancer: Review. *Oncol Rep.* 2010;24:1121-31.
6. Mandal, A. Chemotherapy Principles. *News Medical Life Sciences.* 2017. Available: <https://www.news-medical.net/health/Chemotherapy-Principles.aspx>. [2016, June 11].
7. MM G. Mechanisms of Cancer Drug Resistance. *Annu Rev Med.* 2002;53:615-27.
8. Dingli MA. 2006. Cancer biology: Infectious tumour cells. *Nature.* 443(7107):35-36.
9. Hatzimichael EL, Sim V, Briasoulis E, and Crook T. Epigenetics in Diagnosis, Prognostic Assessment and Treatment of Cancer: An Update. *EXCLI Journal* 2014;13:954-76.
10. Hayflick L. The illusion of cell immortality. *British Journal of Cancer* 2000;83(7):841-6.
11. Hecker E. Definitions and terminology in cancer (tumour) etiology. *Bull World Health Organ, Vol 54, 1976.* 1976;54:1-10.
12. Martinez T, Fultz KE, Ignatenko NA, and Gerner EW. *Molecular Biology of Cancer. Burger's Medicinal Chemistry and Drug Discovery.* Tuscon, Arizona: Wiley&Sons, Inc; 2003.
13. Hejmadi M. *Introduction to Cancer Biology: Momna Hejmadi & Ventus Publishing Aps; 2010.*
14. Rollins GT, Polyak K, and Stiles CD. Molecular biology. In: Holland JF, Frei E, editors. *Cancer medicine.* 5th ed. London: B.C. Decker Inc. Hamilton; 2000. p. 116-46.
15. Vineis PD. Definition and classification of cancer: Monothetic or polythetic? . *Theoretical Medicine.* 1993;14(3):29-256.
16. Bachar RA, Gilat H, Feinmesser R, and Hardy B. Apoptosis and cell surface GRP78 expression in benign and malignant parotid gland tumors. *Head Neck Oncol* 2014;6(2):15.
17. Walker ME, Salesky JS, and Murphey MD. 2011. Magnetic Resonance Imaging of Benign Soft Tissue Neoplasms in Adults. *Radiol Clin N Am.* 49(2011):1197–1217.

18. Ramesh NA, Kusum N, Kiran A, Ashok A, and Somdutt S. Overview of Benign and Malignant Tumours of Female Genital Tract. *Journal of Applied Pharmaceutical Science* 2013;3(1):140-9.
19. Alison WR. 2001. Cancer. *ENCYCLOPEDIA OF LIFE SCIENCES. ENCYCLOPEDIA OF LIFE SCIENCES*. London, UK: Nature Publishing Group; 2001.
20. Friberg SM. On the Growth Rates of Human Malignant Tumors: Implications for Medical Decision Making. *Journal of Surgical Oncology* 1997;65:284-97.
21. Seyfried LM. Cancer as a metabolic disease. *Nutrition & Metabolism*. 2010;7(7):1-22.
22. Dancey PL, Onetto N, and Hudson TJ. The Genetic Basis for Cancer Treatment Decisions. *Cell*. 2012;148:409-20.
23. Regoes RR. Population genetics meets cancer genomics. *PNAS*. 2010;107(43):18241–2.
24. Baeissa HG, Richardson CJ, and Pearl FMG. Mutational patterns in oncogenes and tumour suppressors. *Biochemical Society Transactions* 2016;44(3):925-31.
25. Vogelstein KW. Cancer genes and the pathways they control. *Nat Med*. 2004;10:789-99.
26. Young KA, Edwards JG, and Smith ST. Basic principles of cancer genetics. *J S C Med Assoc*. 1998;94(7):299-305.
27. Knudson AG. Two genetic hits to cancer. *Nature Rev Cancer* 2001;1:157-62.
28. Loescher LW, Traning A, Masny A, and Jenkins J. Genetics in Oncology Practice: Cancer Risk Assessment. *The biology of cancer*. Pittsburgh, PA: Oncology Nursing Society; 2003. p. 23-56.
29. Frank SA. Genetic Predisposition to Cancer — Insights From Population Genetics. *Nature* 2004;5:764-72.
30. Ponder BAJ. Cancer genetics. *NATURE* 2001;4(11):336-41.
31. Miremedi MZ, Pharoah PDP, and Caldas C. Cancer genetics of epigenetic genes. *Human Molecular Genetics* 2007;16(1):28-49.
32. Michor FY, and Nowak MA. Dynamics of Cancer Progression. *Nature Review Cancer*. 2004;4:197-205.
33. Chial H. Proto-oncogenes to oncogenes to cancer. *Nature Education* 2008;1(1):33.
34. Park M. The Genetic Basis of Human Cancer. In: Vogelstein BaK, K. , editor. *Oncogenes*. New York, NY: McGraw-Hill; 1998. p. 205-28.
35. Rice HB, Handley C, and Hall M. Oncogenes and Tumor Suppressor Genes: An Essential Building Block of Cancer. *The Chemist*. 2014;87(2):15-8.
36. Shortt RW. Oncogenes in Cell Survival and Cell Death. *Cold Spring Harb Perspect Biol*. 2012;4:1-11.

37. Hunt K. Fundamentals of Cancer Prevention. In: Alberts DH, L., editor. Hereditary risk for cancer Berlin, Germany: Springer; 2005. p. 61-83.
38. Konopka JW, Singer JW, Collins SJ, and Witte ON. Cell lines and clinical isolates derived from Ph1-positive chronic myelogenous leukemia patients express c-abl proteins with a common structural alteration. *Proc Natl Acad Sci*. 1985;82:1810-4.
39. Devi PU. Basics of Carcinogenesis. *Health Administrator*. 2002;17(1):16-24.
40. Land HP, and Weinberg, RA. Cellular oncogenes and multi-step carcinogenesis. *Science*. 1983;222:771-8.
41. Lowe CE, and Evan G. Intrinsic tumour suppression. *Nature*. 2004;432:307-3015.
42. Cooper GM. *The Cell: A Molecular Approach*. 2000. In: *Tumor Suppressor Genes* Sunderland (MA): Sinauer Associates. 2nd edition.
43. Wilbur B. *The World of the Cell* 7th ed ed. San Francisco, C2009.
44. Kugoh HT, and Oshimura M. Review: Studies of Tumor Suppressor Genes via Chromosome Engineering. *Cancers*. 2016;8(1):4.
45. Rudin C. *The Genetic Basis of Human Cancer*. Vogelstein BaK, K., editor. New York, NY: McGraw-Hill, ; 1998.
46. Sherr CJ. Principles of tumor suppression. *Cell* 2004;116:235-46.
47. Krug UGA and Koeffler HP. Tumor suppressor genes in normal and malignant hematopoiesis. *Oncogene*. 2002;21:3475-95.
48. Yang JCL, Kong X, Huang T, and Cai YD. Analysis of Tumor Suppressor Genes Based on Gene Ontology and the KEGG Pathway. *PLoS ONE*. 2014;9(9).
49. Fearon E. *Tumor suppressor genes*. Vogelstein BaK, K., editor. New York, NY: McGraw-Hill, ; 1998.
50. Chow AY. Cell cycle control by oncogenes and tumor suppressors: driving the transformation of normal cells into cancerous cells. . *Nature Education*. 2010;3:7-8.
51. Zhu KLQ, Zhou Y, Tao C, Zhao Z, and Sun J. Oncogenes and tumor suppressor genes: comparative genomics and network perspectives. *BMC Genomics*. 2015;16(7).
52. Aktipis CMN. Evolutionary foundations for cancer biology. *Evolutionary Applications* 2012;6:144-59.
53. Paul CW, Davies LD, and Tuszynski JA. Cancer as a dynamical phase transition. *Theoretical Biology and Medical Modelling*. 2011;8(30):1-16.
54. DeBerardinis RJ, Lum JJ, Hatzivassiliou G, and Thompson CB. The Biology of Cancer: Metabolic Reprogramming Fuels Cell Growth and Proliferation. *Cell Metabolism*. 2008;7:11-20.

55. Alberts BJA, Lewis J, Raff M, Roberts K, and Walter P. *Molecular Biology of the Cell*; Fourth Edition. 23. Cancer. Garland Science; NY. *Molecular Biology of the Cell*. NY: Garland Science; 2002.
56. Evan KH. Proliferation, cell cycle and apoptosis in cancer. *Nature*. 2001;411(6835):342-8.
57. McDonald AB, and Dedhar S. Integrin-linked kinase – essential roles in physiology and cancer biology. *Journal of Cell Science*. 2008;121(19):3121-32.
58. Klein C. Cancer: The metastasis cascade. *Science*. 2008;321:1785-87.
59. Newton J, Bethel K, Bazhenova L, Nieva J, Norton L, and Kuhn P. Spreaders and Sponges Define Metastasis in Lung Cancer: A Markov Chain Monte Carlo Mathematical Model. *Cancer Research*. 2013;73(9): 2760–9.
60. Psaila BD. The metastatic niche: adapting the foreign soil. *Nature reviews Cancer* 2009;9:285-93.
61. Steeg PS. Targeting metastasis. *Nature Reviews Cancer* 2016;16:201-18.
62. Kanwal S. Effect of O-GlcNAcylation on tamoxifen sensitivity in breast cancer derived MCF-7 cells. 2013.
63. Mehlen P, and Puisieux A. Metastasis: a question of life or death. *Nat Rev Cancer*. 2006;6(6):449-58.
64. Quail JA. Microenvironmental regulation of tumor progression and metastasis. *Nat Med* 2013;19(11):1423-37.
65. Vellai TG. The origin of eukaryotes: the difference between prokaryotic and eukaryotic cells. *The royal society*. 1999; 266:1571-1577.
66. Norris VR. The Eukaryotic Cell Originated in the Integration and Redistribution of Hyperstructures from Communities. 2009; 10:2611-2632.
67. Baum DA, and Baum B. An inside-out origin for the eukaryotic cell. *BMC Biology*. 2014;12(1):76.
68. Holy J, and Perkins E. Structure and Function of the Nucleus and Cell Organelles. In: Krawetz S, editor. *Bioinformatics for Systems Biology*. Totowa, NJ: Humana Press; 2009. p. 3-31.
69. Lim CT, Zhou EH, and Quek ST. Mechanical models for living cells--a review. *Journal of Biomechanics*. 2006;39(2):195-216.
70. Shier DJ, and Lewis R. *Hole's Human Anatomy and Physiology*. 12th ed. New York: McGraw Hill; 2010.
71. Moeendarbary E, Valon L, Fritzsche M, Harris AR, Dale A, Moulding AJ, Thrasher ES, Mahadevan L, and Guillaume T. The cytoplasm of living cells behaves as a poroelastic material. *Nature Materials*. 2013;12:253-61.
72. Fruleux J. 2016. Physical role for the nucleus in cell migration. *Journal of Physics: Condensed Matter*. 28:1-12.

73. Weiss L. *Fundamental Aspects of Metastasis*. North-Holland Publishing Company; 1976.
74. Jiang G, Huang AH, Cai Y, Tanase M, and Sheetz MP. Rigidity sensing at the leading edge through avb3 Integrins and RPTPa. *Biophys J*. 2008;90:1804-9.
75. Gardel ML, Nakamura F, Hartwig J, Crocker JC, Stossel TP, and Weitz DA. Stressdependent elasticity of composite actin networks as a model for cell behavior. *Physical Review Letters*. 2006;96(8):0088102.
76. Gisler T, and Weitz D. Scaling of the Microrheology of Semidilute F-Actin Solutions. *Physical Review Letters*. 1999;82(7):1606-9.
77. Mason T, Gisler T, Kroy K, Frey E, and Weitz D. Rheology of F-actin solutions determined from thermally driven tracer motion. *Journal of Rheology*. 2000;44:917.
78. Van Citters KM, Hoffman, BD, Massiera G, and Crocker JC. The role of F-actin and myosin in epithelial cell rheology. *Biophysical journal*. 2006;91(10):3946-56.
79. Tseng Y, Kole TP, Lee SHJ, and Wirtz D. Local dynamics and viscoelastic properties of cell biological systems. *Current Opinion in Colloid & Interface Science*. 2002;7(3-4):210-7.
80. Tseng YK, and Wirtz D. 2002. Micromechanical Mapping of Live Cells by Multiple-Particle-Tracking Microrheology. *Biophysical Journal*. 83:3162–3176.
81. Jacobs CR, Huang H, and Kwon RY. *Introduction to Cell Mechanics and Mechanobiology*. Garland Science. 2012.
82. Pelling AE, and Horton MA. An historical perspective on cell mechanics. *Pflugers Archiv : European journal of physiology*. 2008;456(1):3-12.
83. Mak RD and Zaman MH. Impact of Dimensionality and Network Disruption on Microrheology of Cancer Cells in 3D Environments. *PLOS Computational Biology*. 2014;10(11):1-12.
84. Nematbakhsh Y, and Lim CT. Cell biomechanics and its applications in human disease diagnosis. *Acta Mechanica Sinica*. 2015;31(2):268-73.
85. Pachenari SM, Janmaleki M, Babazadeh S, Taranejoo S, and Hosseinkhani H. Mechanical properties of cancer cytoskeleton depend on actin filaments to microtubules content: investigating different grades of colon cancer cell lines. *J Biomech*. 2014;47(2):373-9.
86. Nematbakhsh CT. Cell biomechanics and its applications in human disease diagnosis. *Acta Mechanica Sinica*. 2015;31(2):268-73.
87. Mansel BW. A Practical Review of Microrheological Techniques. *A Practical Review of Microrheological Techniques* 2(1):1–21.
88. Ewesuedo RB, and Ratain MJ. Principles of Cancer Chemotherapy. In: Vokes EE, Golomb HM, editors. *Oncologic Therapies*. Berlin, Heidelberg: Springer Berlin Heidelberg; 2003. p. 19-66.

89. Gatti LF. Overview of tumor cell chemoresistance mechanisms. *Methods Mol Med*. 111:127-148.
90. Liu FM. Mechanisms of Chemotherapeutic Drug Resistance in Cancer Therapy—A Quick Review. *Taiwan J Obstet Gynecol*. 2009;43(3):239-44.
91. Hunt TNK, and Novák B. The cell cycle. *Philosophical Transactions of the Royal Society B: Biological Sciences*. 2011;366(1584):3494-7.
92. Behl C. Cell Aging: Molecular Mechanisms and Implications for Disease. *SpringerBriefs in Molecular Medicine*. 2014;49(108):9-19.
93. Imoto YY, Yagisawa F, Kuroiw H, and Kuroiwa T. The cell cycle, including the mitotic cycle and organelle division cycles, as revealed by cytological observations. *Journal of Electron Microscopy*. 2011;60(1):117-36.
94. Kar S. *Unraveling Cell-Cycle Dynamics in Cancer*. India: Elsevier Inc. 2016; 2(1):8-10.
95. Renthal WE. Cancer and the role of cell cycle checkpoints. *Reviews in Undergraduate Research*. 2002;1:1-7.
96. Lodish HB, Zipursky LS, Matsudaira P, Baltimore D, and Darnell J. *Molecular Cell Biology*. New York: W. H. Freeman and Company; 2000.
97. Cross FE, and Skotheim JM. Evolution of networks and sequences in eukaryotic cell cycle control. *Phil Trans R Soc B*. 2011;366:3532-44.
98. Williams GHK. The cell cycle and cancer. *J Pathol* 2012;226:352-64.
99. Meunier SI. Acentrosomal Microtubule Assembly in Mitosis: The Where, When, and How. *Trends in Cell Biology*. 2016;26(2):80-7.
100. Ohkura H. *Meiosis: An Overview of Key Differences from Mitosis*. . 2016. United Kingdom: Cold Spring Harbor Laboratory Press.
101. Clarke DJ. Mitosis: Introduction. *Cell Cycle*. 2002;1(5):298-9.
102. Gavhane YS, Bhagat AK, Shinde VR, Bhong KK, Khairnar GA, and Yadav AV. Solid Tumors: Facts, Challenges and Solutions. *International Journal of Pharma Sciences and Research*. 2011; 2(1): 1-12.
103. Schwartz GMA. Targeting the cell cycle: a new approach to cancer therapy. *J Clin Oncol* 200;23:9408-21.
104. Bailar JHL. Cancer undefeated. . *N Engl J Med* 1997;336:1569-74.
105. Gardner SN. Cell Cycle Phase-Specific CHEmotherapy: Computation Methods for Guiding Treatment. *Cell Cycle*. 2002;1(6):369-74.
106. Fister JCP. *Optimal Control Applied to Cell-Cycle-Specific Cancer Chemotherapy*. Society for Industrial and Applied Mathematics. 2000;60(3):1059-72.

107. Powathil GM, and Swat M. Investigating the development of chemotherapeutic drug resistance in cancer: A multiscale computational study. *IET Systems Biology*. 2014;1:1-13.
108. Ozawa SS, Mitsuhashi Y, Kobayashi T, and Inaba M. Cell killing action of cell cycle phase-non-specific antitumor agents is dependent on concentration--time product. *Cancer Chemother Pharmacol*. 1988;21(3):185-90.
109. Cheung-Ong KG, and Nislow C. DNA-damaging agents in cancer chemotherapy: serendipity and chemical biology. *Chem Biol* 2013;20(5):648-59.
110. Housman GB, Heerboth S, Lapinska K, Longacre M, Snyder N, and Sarkar S. Drug Resistance in Cancer: An Overview. *Cancer*. 2014;6:1769-1792.
111. Cunningham JJ, Gatenby RA, and Brown JS. Evolutionary dynamics in cancer therapy. *Mol Pharm*. 2011;8:2094-100.
112. Cornelison RL, and Landen CN. Emerging Therapeutics to Overcome Chemoresistance in Epithelial Ovarian Cancer: A Mini-Review. *Int J Mol Sci* 2017;18:2171.
113. Ojini IA. Rapid Identification of Chemoresistance Mechanisms Using Yeast DNA Mismatch Repair Mutants. *Biochemistry*. 2015;5:1925-35.
114. Selvaggi LS, Vaccaro C, Pesce G, Rusciano G, Sasso A, Campanella C, and Carotenuto R. Multiple-Particle-Tracking to investigate viscoelastic properties in living cells. *Methods*. 2010; 51(1):20-26.
115. Schultz EM. Microrheology of biomaterial hydrogelators. *Soft matter*. 2012;8(23):6198-205.
116. Crocker JC. Two-Point Microrheology of Inhomogeneous Soft Materials. *The American Physical Society*. 2000;85(4):888-91.
117. Blair DE. The Matlab Particle Tracking Code Repository. 2011.
118. Wirtz D. Particle-Tracking Microrheology of Living Cells: Principles and Applications. *Annu Rev Biophys*. 2009;38:301-26.
119. Livak TD. Analysis of relative gene expression data using real-time quantitative PCR and the 2(-Delta Delta C(T)) Method. *Methods Mol Med*. 2001;24(5):402-8.
120. Siddik ZH. Cisplatin: mode of cytotoxic action and molecular basis of resistance. *Oncogene*. 2003;22(47):7265-79.
121. Galluzzi L. Molecular mechanisms of cisplatin resistance. *Oncogene*. 2012;31(15):1869-83.
122. Guarnieri D, Falanga A, Fusco S, Belli V, and Perillo E. Surface decoration with gH625-membranotropic peptides as a method to escape the endo-lysosomal compartment and reduce nanoparticle toxicity. *Nanotechnology*. 2015;26(41):415101.
123. Levental KR YH, Kass L, Lakins JN, Egeblad M, and Ertler JT. Matrix Crosslinking Forces Tumor Progression by Enhancing Integrin Signaling. *Cell*. 2009;139(5):891-906.

124. Li WY, Schimmel N, Al-Ameen MA, and Ghosh G. Breast cancer cells mechanosensing in engineered matrices: Correlation with aggressive phenotype. *J Mech Behav Biomed Mater.* 2016;61:208-20.
125. Hoffman BD, Van Citters KM, and Crocker JC. The consensus mechanics of cultured mammalian cells. *Proc Natl Acad Sci.* 2006;103(27):10259-64.
126. Tian M LY, Liu W, Jin L, Jiang X, and Wang X. The nanomechanical signature of liver cancer tissues and its molecular origin. *Nanoscale.* 2015;7(30):12998-3010.
127. Li MD. Cisplatin regulates the MAPK kinase pathway to induce increased expression of DNA repair gene ERCC1 and increase melanoma chemoresistance. *Oncogene.* 2012;31:2412-22.
128. Bhatia TS, and Thompson JA. Treatment of metastatic melanoma: an overview. *Oncology.* 2009;23:488-96.
129. De Souza CF, and Jasiulionis MG. Biomarkers as key contributors in treating malignant melanoma metastases. *Dermatol Res Pract* 2012;2012(1-4).
130. Bruehlmann SB, Matyas JR, and Duncan NA. Regional variations in the cellular matrix of the annulus fibrosus of the intervertebral disc. *J Anat.* 2002;201:159-71.
131. Johnson WE. Human intervertebral disc cell morphology and cytoskeletal composition: a preliminary study of regional variations in health and disease. *J Anat.* 2003;203:605-12.
132. Berret JF. Local viscoelasticity of living cells measured by rotational magnetic spectroscopy. *Nat Commun.* 2016;7:10134.
133. Hecht FM. Imaging viscoelastic properties of live cells by AFM: power-law rheology on the nanoscale. *Soft Matter* 2015;11(23):4584-91.
134. Cia P. Quantifying cell-to-cell variation in power-law rheology. *Biophys J* 2013;105(5):1093-102.
135. Rigato A, Eghiaian F, Piel M, and Scheuring S. Atomic Force Microscopy Mechanical Mapping of Micropatterned Cells Shows Adhesion Geometry-Dependent Mechanical Response on Local and Global Scales. *ACS Nano* 2015;9(6):5846-56.
136. Park CY. Mapping the cytoskeletal prestress. *Am J Physiol Cell Physiol* 2010;298(5):1245-52.
137. Brangwynne CP, MacKintosh FC, and Weitz DA. Intracellular transport by active diffusion. *Trends Cell Biol.* 2009;19(9):423-7.
138. Dominguez KC. Actin Structure and Function. *Annu Rev Biophys.* 2011;9(40):169-86.
139. Cepeda V, Castilla J, Alonso C, Quevedo C, and Perez JM. Biochemical mechanisms of cisplatin cytotoxicity *Anticancer Agents Med Chem.* 2007;7:3-8.
140. Wexselblatt EY, and Gibson D. Cellular interaction of platinum drugs. *InorganicChim Acta.* 2012;396:75-83.

141. Li S DV, and Blain EJ. Zonal variations in cytoskeletal element organisation, mRNA and protein expression in the intervertebral disc. *J Anat.* 2008;213:725-32.
142. Hadnagy A, and Balicki D. Histone tail modifications and non-canonical functions of histones: perspectives in cancer epigenetics. *Mol Cancer Ther.* 2008;7:740-8.
143. Foroodi DW, and Singh G. Interactions of doxycycline with chemotherapeutic agents in human breast adenocarcinoma MDA-Mb-231 cells. *Anticancer Drugs.* 2009;20:115-22.
144. Wang Q, Han C, Huang YW, Wani G, and Thomale J. Differential contributory roles of nucleotide excision and homologous recombination repair for enhancing cisplatin sensitivity in human ovarian cancer cells. *Mol Cancer Ther.* 2011;10:10-24.
145. Milrot E, Flescher E, Gonen P, Kelson I, and Heisari Y. Enhancing killing of cervical cancer cells by combinations of methyl jasmonate with cisplatin, X or alpha radiation. *Invest New Drugs.* 2012;31:333-44.
146. Waigh TA. Microrheology of complex fluids. *Reports on Progress in Physics.* 2005;68(3):685-742.
147. Valentine M, Kaplan P, Thota D, Crocker J, Gisler T, and Prud'homme R. Investigating the microenvironments of inhomogeneous soft materials with multiple particle tracking. *Physical Review E.* 2006;64(6):61506.

APPENDICES

Appendix A: MSK Human Specimen MTA



AGREEMENT FOR INTER-INSTITUTIONAL TRANSFER OF HUMAN TISSUE SAMPLES

Between
ACADEMIC COLLEAGUES
("Agreement")

MSK00005691

1. Memorial Sloan Kettering Cancer Center ("MSK") and University of Cape Town ("INSTITUTION") agree that MSK will provide INSTITUTION with SK-MEL-29 ("SAMPLES") derived from human subjects under approved IRB protocol number 00-144.
2. SAMPLES and any related confidential information, including but not limited to, all non-public, confidential or proprietary information that MSK designated or otherwise marked as "Confidential" ("INFORMATION") will be sent by Dr. Taha Merghoub of MSK ("INVESTIGATOR") to INSTITUTION.
3. INSTITUTION shall use SAMPLES and INFORMATION for the following purpose: **Cell Mechanics in Chemoresistance of Malignant Melanoma** ("STUDY") as described in Exhibit A.
4. MSK retains ownership of SAMPLES and INFORMATION and may distribute SAMPLES and INFORMATION to other commercial or non-commercial entities.
5. INSTITUTION will NOT use SAMPLES in humans.
6. INSTITUTION shall not transfer SAMPLES or INFORMATION to any non-INSTITUTION person without prior written consent from MSK.
7. INSTITUTION represents that its use of SAMPLES and INFORMATION will be in compliance with all applicable laws and regulations.
8. INSTITUTION agrees that the SAMPLES and INFORMATION shall not be used, directly or indirectly, for any commercial purpose, including filing patent applications thereon, but only for the STUDY described above.
9. INSTITUTION agrees to hold in confidence for a period of three (3) years after receipt, all INFORMATION received from MSK under this Agreement, except for information which:
 - a) was lawfully in INSTITUTION's possession or control prior to the date of disclosure as evidenced by written records; or
 - b) was in the public domain or enters into the public domain through no improper act on INSTITUTION's part or on the part of any of INSTITUTION's employees;
 - c) is rightfully given to INSTITUTION from sources independent of MSK; or
 - d) is independently developed by INSTITUTION, as evidenced by written records; or
 - e) must be disclosed for minimum lawful compliance with court orders, regulations and statutes.
10. INSTITUTION will report all RESULTS to INVESTIGATOR. "RESULTS" shall mean all findings, data, work products, results and other information generated from the STUDY using the SAMPLES and/or INFORMATION. MSK and INSTITUTION will jointly publish, and each party may use RESULTS for any internal non-commercial research or educational purpose. INSTITUTION agrees any publication or presentation of RESULTS will acknowledge MSK and INVESTIGATOR as source of SAMPLES, and cite any scientific contribution of the INVESTIGATOR.
11. INSTITUTION shall not use the name of Memorial Sloan-Kettering Cancer Center, Memorial Hospital for Cancer and Allied Diseases or Sloan-Kettering Institute for Cancer Research, or a variant of any of the foregoing in any advertising or publicity matter without the prior written approval of MSK, except as set forth in Article 10.
12. MSK will make all attempts to ensure that any information revealing the identity of the patients contributing the SAMPLES will be removed from INFORMATION. INSTITUTION agrees to make best efforts to erase and remove any such identifying information that may remain despite MSK's precautions.

I | Page

MSK NON-PROFIT HUMAN SPECIMEN MTA

13. SAMPLES are being provided by MSK "AS IS" WITHOUT ANY WARRANTIES, EXPRESSED OR IMPLIED, INCLUDING ANY WARRANTY OF FITNESS FOR A PARTICULAR PURPOSE. MSK MAKES NO REPRESENTATION THAT THE USE OF THE SAMPLES WILL NOT INFRINGE ANY PATENT, COPYRIGHT, TRADEMARK OR OTHER PROPRIETARY RIGHT.
14. In no event shall MSK be liable for any use by INSTITUTION of SAMPLES or for any loss, claim, damage, or liability, of any kind or nature that may arise from or in connection with this Agreement or the use, handling, or storage of SAMPLES. INSTITUTION agrees to assume all liability for damages that arise from its use, storage or disposal of SAMPLES, except to the extent such liability is due to MSK's gross negligence or willful misconduct.
15. INSTITUTION will reimburse MSK \$300.00 for costs associated with the preparation and shipping SAMPLES.
16. The Agreement will terminate on the earlier of its second (2nd) anniversary or upon thirty (30) days prior written notice of one party to the other, in which case INSTITUTION will discontinue within thirty (30) days its use of SAMPLES. INSTITUTION agrees, upon direction of INVESTIGATOR, to return or destroy SAMPLES upon termination of this Agreement.
17. This Agreement may not be assigned by INSTITUTION without the prior written consent of MSK.
18. Articles 2, 4, 6, 8-11, 13 and 14 will survive the termination of this Agreement.
19. An authorized representative of each party must sign this Agreement. The Agreement is effective the date of the last signature below ("Effective Date").

UNIVERSITY OF CAPE TOWN

By: _____
 Name: WARDA SABLAY
 Contracts Manager
 Research Contracts & Innovation
 University of Cape Town
 Title: _____
 Date: 19 June 2017

MEMORIAL SLOAN KETTERING CANCER CENTER

By: _____
 Name: Lawrence Lupkin, MPA
 Title: Senior Manager, Operations & Finance
 Office of Technology Development
 Date: 6/20/17

INSTITUTION Investigator acknowledges that she/he has read, understands and accepts her/his obligations under this Agreement:

Investigator's signature: _____
 Name: Dr. Thomas Franz
 Date: 19 June 2017

Signatures Removed

Exhibit A:

Description of Study

This study aims at investigating whether the mechanical properties (stiffness) of cancer cells can serve as a diagnostic marker for drug resistance. We wish to assess whether, and if so to what degree, cell stiffness is affected by drug exposure. We wish to compare non-recurrent and recurrent melanoma cells. We have access to a non-recurrent melanoma line in-house.

Study Design

STAGE 1:

Purpose: To examine the mechanical and cellular properties of malignant melanoma cells before chemo exposure.

Cell Culture: Malignant Melanoma cell line (in-house), non-chemo control

Testing:

1. qRT-PCR
2. Western blot
3. Microrheology: To determine mechanical properties by particle tracking using β -tubulin

STAGE 2:

Purpose: To examine the mechanical and cellular properties of malignant melanoma cells post chemo exposure.

Cell Culture: Malignant Melanoma cell line (in-house), Exposed to Chemotherapeutic agent = Cisplatin

Testing:

1. qRT-PCR
2. Western blot
3. Cell Viability: MTT Assay or Alamar Blue Assay
4. Microrheology: To determine mechanical properties by particle tracking

STAGE 3:

Purpose: To examine the mechanical and cellular properties of recurrent malignant melanoma cells (chemo-resistant).

Cell Culture: Recurrent Malignant Melanoma cell line (**SK-MEL-29**), No chemo treatment

Exhibit A:

Description of Study

This study aims at investigating whether the mechanical properties (stiffness) of cancer cells can serve as a diagnostic marker for drug resistance. We wish to assess whether, and if so to what degree, cell stiffness is affected by drug exposure. We wish to compare non-recurrent and recurrent melanoma cells. We have access to a non-recurrent melanoma line in-house.

Study Design

STAGE 1:

Purpose: To examine the mechanical and cellular properties of malignant melanoma cells before chemo exposure.

Cell Culture: Malignant Melanoma cell line (in-house), non-chemo control

Testing:

1. qRT-PCR
2. Western blot
3. Microrheology: To determine mechanical properties by particle tracking using β -tubulin

STAGE 2:

Purpose: To examine the mechanical and cellular properties of malignant melanoma cells post chemo exposure.

Cell Culture: Malignant Melanoma cell line (in-house), Exposed to Chemotherapeutic agent = Cisplatin

Testing:

1. qRT-PCR
2. Western blot
3. Cell Viability: MTT Assay or Alamar Blue Assay
4. Microrheology: To determine mechanical properties by particle tracking

STAGE 3:

Purpose: To examine the mechanical and cellular properties of recurrent malignant melanoma cells (chemo-resistant).

Cell Culture: Recurrent Malignant Melanoma cell line (**SK-MEL-29**), No chemo treatment

Testing:

1. qRT-PCR

2. Western blot

3. Microrheology: To determine mechanical properties by particle tracking

Appendix B: Reagents Lists

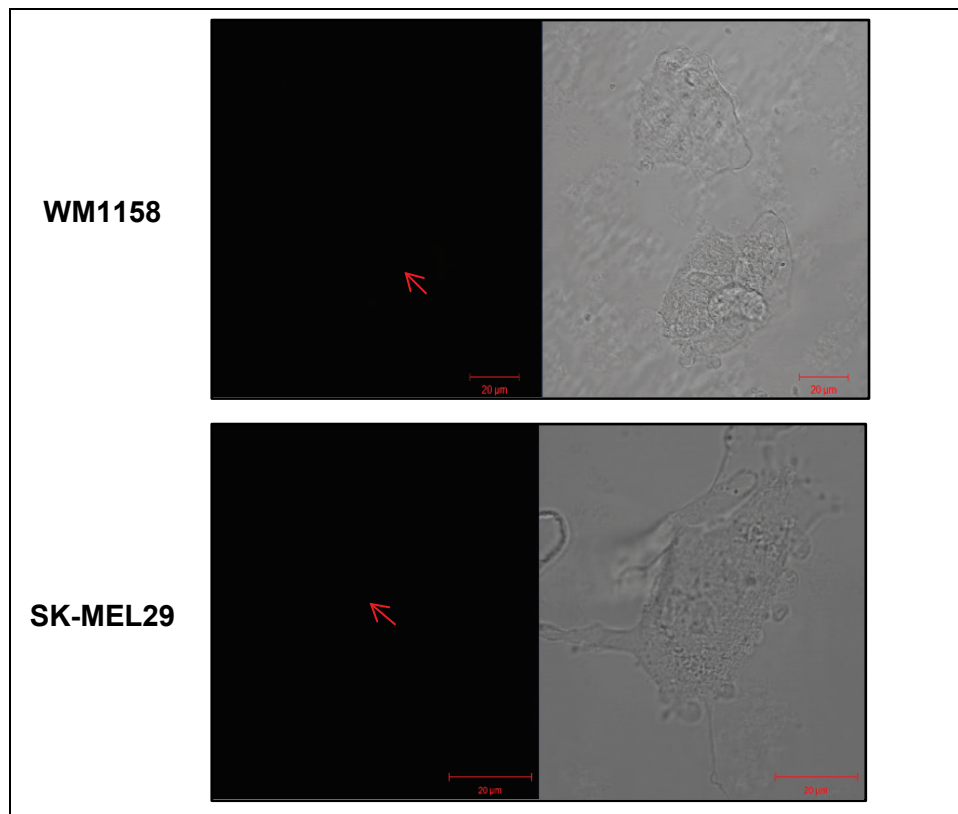
Table 8: Regularly used reagents and substances.

Reagents	Manufacturer
2-Mercaptoethanol	Sigma-Aldrich, USA
Acrylamide solution 40%	Sigma-Aldrich, USA
Ammonium persulfate–APS	Sigma-Aldrich, USA
Bromophenol Blue	Sigma-Aldrich, USA
Ethanol	Sigma-Aldrich, USA
Potassium chloride – KCl	Merck- Calbiochem, USA
Methanol	Merck-Millipore, USA
MgCl ₂ – Magnesium chloride	Merck- Calbiochem, USA
<i>N,N,N',N'</i> -Tetramethylethylenediamine (TEMED)	Sigma-Aldrich, USA
Ponceau S	Sigma-Aldrich, USA
Sodium acetate	Sigma-Aldrich, USA
Sodium chloride –NaCl	Merck- Calbiochem, USA
Sodium Dodecyl Sulphate (SDS)	Sigma-Aldrich, USA
Tween 20™	Sigma-Aldrich, USA
Trypsin	Sigma-Aldrich, USA
Hydrochloric acid 32% - HCl	Merck- Millipore, USA

Table 9: Sample Loading Buffer (2X).

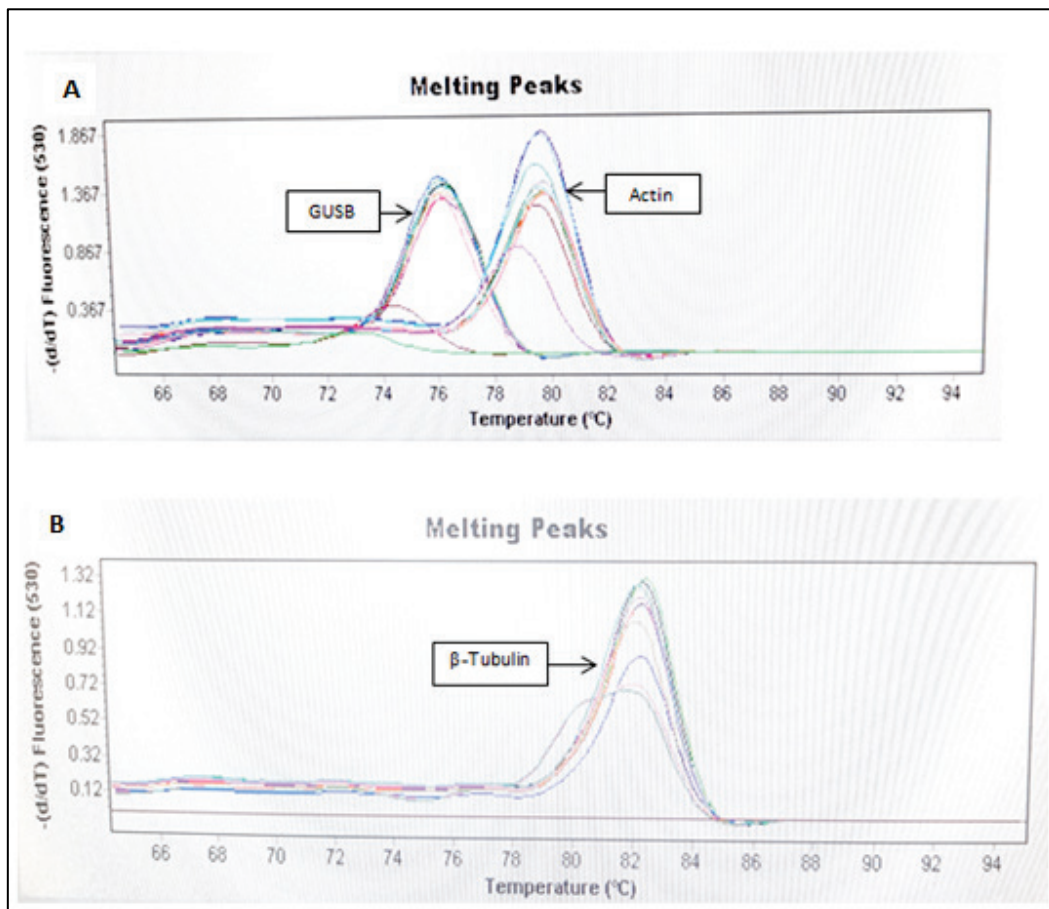
Reagents	Concentration
dH ₂ O	1.75 mL
1M Tris-HCL, pH6.8	1.25 mL
10% SDS	4 mL
Glycerol	2 mL
Bromophenol blue	0.05 mg
β-mercaptoethanol	1 mL

Appendix C: Negative controls microrheology (MPTM)



Negative controls used for MPTM testing was performed to determine the presence or absence of MitoTracker in the cell culture plates. For our control no MitoTracker was added, as observed below there is no green fluorescence visible, indicated by the red arrows.

Appendix D: Melting Peak Analysis of Primers for qRT-PCR



A) Line chart illustrating the melting peaks for the target gene (Actin) and the housekeeping gene (GUSB). Melting curve analysis for both WM1158 and SK-MEL29 cell lines is summarised with single melting peaks are observed for both GUSB and ACTC1 primers assayed, indicating high specificity. **B)** Line chart illustrating the melting peaks for the target gene (β -Tubulin), by representing the different cell line conditions by the different colours. Melting curve analysis for both WM1158 and SK-MEL29 cell lines is summarised with single melting peak was observed for TUBB primer assayed, also indicating high specificity. The melt peak describes the temperature at which the synthesized DNA fragment denatures from the cDNA template, representing the melting temperature T_m of the double stranded DNA product. The temperature is plotted against the negative regression of fluorescence, $-(d/dT)$.